Published in final edited form as:
Am J Physiol Cell Physiol. 2012 March 15; 302(6): C853–C867. doi:10.1152/ajpcell.00071.2011.

Constitutive expression of a Mg^{2+}-inhibited K^+ current and a TRPM7-like current in human erythroleukemia cells

Michael J. Mason[1], **Catherine Schaffner**[2], **R. Andres Floto**[2], and **Quok An Teo**[1]

[1]Department of Physiology, Development, and Neuroscience, University of Cambridge, United Kingdom

[2]Cambridge Institute for Medical Research, Addenbrooke's Hospital, Cambridge, United Kingdom

Abstract

Whole cell patch-clamp experiments were undertaken to define the basal K^+ conductance(s) in human erythroleukemia cells and its contribution to the setting of resting membrane potential. Experiments revealed a non-voltage-activated, noninactivating K^+ current. The magnitude of the current recorded under whole cell conditions was inhibited by an increase in free intracellular Mg^{2+} concentration. Activation or inactivation of the Mg^{2+}-inhibited K^+ current (MIP) was paralleled by activation or inactivation of a Mg^{2+}-inhibited TRPM7-like current displaying characteristics indistinguishable from those reported for molecularly identified TRPM7 current. The MIP and TRPM7 currents were inhibited by 5-lipoxygenase inhibitors. However, inhibition of the MIP current was temporally distinct from inhibition of TRPM7 current, allowing for isolation of the MIP current. Isolation of the MIP conductance revealed a current reversing near the K^+ equilibrium potential, indicative of a highly K^+-selective conductance. Consistent with this finding, coactivation of the nonselective cation current TRPM7 and the MIP current following dialysis with nominally Mg^{2+}-free pipette solution resulted in hyperpolarized whole cell reversal potentials, consistent with an important role for the MIP current in the setting of a negative resting membrane potential. The MIP and TRPM7-like conductances were constitutively expressed under in vivo conditions of intracellular Mg^{2+}, as judged by their initial detection and subsequent inactivation following dialysis with a pipette solution containing 5 mM free Mg^{2+}. The MIP current was blocked in a voltage-dependent fashion by extracellular Cs^+ and, to a lesser degree, by Ba^{2+} and was blocked by extracellular La^{3+} and 2-aminoethoxydiphenyl borate. MIP currents were unaffected by blockers of ATP-sensitive K^+ channels, human ether-à-go-go-related gene current, and intermediate-conductance Ca^{2+}-activated K^+ channels. In addition, the MIP current displayed characteristics distinct from conventional inwardly rectifying K^+ channels. A similar current was detected in the leukemic cell line CHRF-288-11, consistent with this current being more generally expressed in cells of leukemic origin.

Address for reprint requests and other correspondence: M. J. Mason, Dept. of Physiology, Development, and Neuroscience, Univ. of Cambridge, Downing St., Cambridge, UK CB2 3EG (mjm39@cam.ac.uk).

DISCLOSURES

No conflicts of interest, financial or otherwise, are declared by the authors.

Europe PMC Funders Author Manuscripts

Keywords

potassium conductance; patch clamp; magnesium

Alterations in ion channel phenotype have been reported in a variety of human cancers (1, 3, 10, 18). For example, loss of the conventional inwardly rectifying K^+ conductance has been reported in a variety of tumor cells of distinct neural origins (3), while suppression of the delayed rectifier-type voltage-activated K^+ conductance has been reported in megakaryocytes from patients with acute myelogenous leukemia (18). Suppression of the voltage-activated K^+ conductance in megakaryocytes correlates with the malignant state, since remission following chemotherapy resulted in the resurrection of voltage-activated K^+ channel function. Furthermore, three leukemic cell lines frequently used as models for many megakaryocyte and platelet functions, DAMI, CHRF-288-11, and human erythroleukemia (HEL) cells, were without detectable delayed rectifier-type voltage-activated K^+ channel activity.

In numerous cancers and cancer cell lines of diverse origins, the downregulation of conventional K^+ conductances is accompanied by the detection of members of the ether-à-go-go (EAG) gene family (3, 6, 29). Expression of EAG1 and a related human correlate, human ether-à-go-go-related gene (hERG), has been reported in a variety of tumor cells and cell lines (3, 7, 12, 25). Upregulation of hERG has also been shown in B-cell chronic lymphocytic leukemia and numerous hematopoietic cell lines of leukemic origin (30, 36).

The loss of conventional K^+ channel function and the upregulation of members of the EAG gene family have important implications for the maintenance of resting membrane potential in malignant cells. Because activation of members of the EAG channel family is voltage-dependent, they are unable to maintain resting membrane potential at hyperpolarized levels, as recorded in their nonmalignant cell counterparts. As such, malignant cells have a depolarized phenotype (3, 18), a characteristic that may contribute to the malignant state. Depolarization has an impact on many physiological processes, including Ca^{2+} entry and volume regulation, processes that may affect cell proliferation, differentiation, and apoptosis. It has been proposed that this depolarized state may facilitate the malignant phenotype by inhibiting electrogenic Ca^{2+} entry, leading to reduced Ca^{2+}-induced cell death and propagation of the malignant phenotype (36).

Although suppression of voltage-activated K^+ channel activity has been reported in megakaryocytes from patients with acute myelogenous leukemia and related leukemic lines such as HEL and CHRF-288-11 cells (18), knowledge of the basal K^+ conductances contributing to the setting of the resting membrane potential in its absence is lacking. The present experiments were undertaken to investigate the basal K^+ conductance(s) in HEL and CHRF-288-11 cells.

MATERIALS AND METHODS

Reagents

NaCl, KCl, $MgCl_2$, $LaCl_3$, HEPES, Na^+-methanesulfonate, K^+-methanesulfonate, *N*-methyl-D-glucamine (NMDG), EGTA, EDTA, *N*-2-hydroxyethyl-EDTA, NH_4Cl, K_2ATP, glutamic acid, NaOH, KOH, and DMSO were purchased from Sigma-Aldrich (Gillingham, Dorset, UK); $CaCl_2$, $MgSO_4$, $BaCl_2$, and potassium acetate from BDH (Poole, Dorset, UK); and glucose from Fissons Scientific Apparatus (Loughborough, Leicestershire, UK). Clotrimazole, glibenclamide, 2-aminoethoxydiphenyl borate (2-APB), and nordihydroguaiaretic acid (NDGA) were purchased from Sigma-Aldrich and made up in DMSO; 2-(12-hydroxydodeca-5,10-diynyl)-3,5,6-trimethyl-1,4-benzoquinone (AA-861) was purchased from Sigma-Aldrich and made up in ethanol; and *N*-[4-[[1-[2-(6-methyl-2-pyridinyl)ethyl]-4-piperidinyl]carbonyl]phenyl] methanesulfonamide dihydrochloride (E-4031) was purchased from Merck Bioscience Calbiochem (Nottingham, UK) and made up in distilled water.

Cell culture

HEL cells, originally obtained from the European Collection of Animal Cell Cultures (Porton Down, Salisbury, UK), and CHRF-288-11 cells, obtained from the laboratory of Tony Green (Cambridge Institute for Medical Research, Cambridge, UK), were propagated in HCO_3^--buffered RPMI 1640 medium supplemented with 10% fetal bovine serum, 4 mM L-glutamine, 100 U/ml penicillin, and 50 μg/ml streptomycin (all from Sigma-Aldrich or Invitrogen, Paisley, UK). Cells were grown at 37°C in a humidified 95% air-5% CO_2 atmosphere. Cells were passaged two to three times per week and normally used 48–72 h thereafter.

Solutions

The standard KCl-based pipette solution (*solution 1*) contained (in mM) 150 KCl, 0.15 EGTA, and 10 HEPES, with pH adjusted to 7.2 with KOH (calculated $[K^+]$ = 154 mM). When required, 1 or 5 mM Mg^{2+} was added directly as the Cl^- or, in some cases, SO_4^{2-} salt. NMDG internal solution (*solution 2*) was made by equimolar substitution of K^+ with NMDG. In some experiments, a Mg^{2+}-free pipette solution containing EGTA and EDTA (*solution 3*; in mM: 150 KCl, 10 EGTA, 0.5 EDTA, and 10 HEPES, with pH adjusted to 7.2 with KOH) was used to activate Mg^{2+}-inhibitable currents. In some experiments, intracellular Ca^{2+} concentration was buffered to defined values. The Ca^{2+}-to-EGTA ratio was determined using WEBMAXC, with Extended Constants written by C. Patton (www.stanford.edu/~cpatton/maxc.html). A whole cell pipette internal solution with 50 nM free Ca^{2+} (*solution 4*) contained (in mM) 150 KCl, 2.267 $CaCl_2$, 10 EGTA, and 10 HEPES, with pH adjusted to 7.2 with KOH, at 22°C. A low-Cl^- internal solution with 170 nM free Ca^{2+} (*solution 5*) contained (in mM) 150 K^+-glutamate, 1 $CaCl_2$, 2 EGTA, and 10 HEPES, with pH adjusted to 7.2, at 22°C. The pipette solution containing 3 mM free ATP (*solution 6*) contained (in mM) 144 KCl, 0.15 EGTA, 3 K_2ATP, and 10 HEPES, with pH adjusted to 7.2, at 22°C. For pipette solutions containing defined MgATP and free Mg^{2+} levels, WEBMAXC with Extended Constants was used to determine the ratio of ATP to Mg^{2+}

added. The solution with 5 mM MgATP and 3 mM free ATP (*solution 7*) contained (in mM) 134 KCl, 0.15 EGTA, 8 K_2ATP, 5.18 $MgCl_2$, and 10 HEPES, with pH adjusted to 7.2, at 22°C. Free Mg^{2+} concentration ($[Mg^{2+}]$) in this solution was calculated to be 184 μM. A pipette solution with 5 mM free Mg^{2+} and 4.9 mM MgATP (*solution 8*) contained (in mM) 140 KCl, 0.15 EGTA, 5 K_2ATP, 9.92 $MgCl_2$, and 10 HEPES, with pH adjusted to 7.2, at 22°C. Free ATP in this solution was calculated to be 109 μM.

The standard extracellular solution (149 Na^+/5 mM K^+) (*solution 9*) contained (in mM) 145 NaCl, 5 KCl, 1 $MgCl_2$, 10 glucose, and 10 HEPES, with pH adjusted to 7.35 with NaOH (calculated $[Na^+]$ = 149 mM). High-K^+ (154 mM K^+) solution (*solution 10*) contained (in mM) 150 KCl, 1 $MgCl_2$, 10 glucose, and 10 HEPES, with pH adjusted to 7.35 with KOH (calculated total $[K^+]$ = 154 mM). Intermediate-K^+ solutions were made by mixing these two solutions. When required, 1 mM $CaCl_2$ or 150 μM EGTA was added directly to these solutions. These extracellular solutions were supplemented with 400 nM clotrimazole to ensure that membrane currents were not contaminated by the endogenous Ca^{2+}-activated K^+ current in HEL cells (M. J. Mason, unpublished observations). Low-Cl^- external solution (*solution 11*) contained (in mM) 145 Na^+-methanesulfonate, 5 K^+-methanesulfonate, 1 $CaCl_2$, 1 $MgSO_4$, 10 glucose, and 10 HEPES, with pH adjusted to 7.35 with NaOH. Cl^--free solutions were supplemented with 200 nM clotrimazole. Divalent ion-free saline solution (*solution 12*) contained (in mM) 145 NaCl, 5 KCl, 10 *N*-2-hydroxyethyl-EDTA, 10 glucose, and 10 HEPES, with pH adjusted to 7.35 with NaOH, and was supplemented with 200 nM clotrimazole. In some experiments, clotrimazole was omitted from the extracellular solutions as noted in the text. All extracellular solution changes were made by gravity-fed superfusion.

Patch-clamp measurements

Cells were added to a low-volume Plexiglas chamber mounted on the stage of an inverted microscope. The bottom of the chamber was formed by adherence of a glass coverslip with silicone grease. The chamber was grounded via a Ag-AgCl pellet placed directly in the chamber downstream of the cells. Tight-seal whole cell patch-clamp recordings in voltage-clamp mode were carried out using an Axopatch 200A amplifier (Molecular Devices, Sunnyvale, CA). The series resistance compensation feature of the amplifier was used to achieve 70% series resistance compensation. Electrodes were pulled from filamented borosilicate glass (Harvard Apparatus, Kent, UK), and the tips were fire polished. Electrodes had resistances of 2–8 MΩ when filled with standard KCl-based internal solution. All experiments were performed at room temperature (20–24°C).

Amplifier control and data acquisition were performed using Axograph 4.9 software (Axograph Scientific, Sydney, Australia) running on a Macintosh computer using a Digidata 1322A 16-bit data acquisition system (Molecular Devices). For recording of whole cell ramp currents under voltage clamp, cells were held at 0, −20, or −80 mV, and 200-ms ramps from −100 to +100 mV were initiated every 1 or 3 s (these voltages are uncorrected for junction potential errors). Currents were filtered at 1 kHz and acquired to disk at 2 kHz. In a small number of experiments, data were acquired at 10 kHz. Currents at −90, 0, and +90 mV were calculated as 3-point averages extracted from individual voltage ramps using custom macros

written in IGOR Pro (Wavemetrics, Lake Oswego, OR). Reversal potentials, measured from voltage ramp data using analysis software within Axograph, were averaged over five consecutive ramps.

A voltage-step protocol was employed for investigations of voltage- and time-dependent current activation. Cells were held at 0 or −80 mV, and 500-ms steps to voltages between −100 and +100 mV were initiated in 20-mV increments (these voltages are uncorrected for junction potential errors). Mean step currents recorded during 500-ms voltage steps were averaged between 5 and 495 ms of the voltage step.

For experiments initiated with KCl-based pipette solutions and NaCl-based extracellular solutions, a +3-mV junction potential correction was applied to all voltages (27). Experiments using Cl^--free internal solution and Cl^--containing extracellular solution have been corrected for a +10-mV junction potential error (27), while experiments using an NMDG-based internal solution have been corrected for a −6-mV junction potential error (28). Data acquired during acetate application have been corrected for a junction potential error arising from exposure of the Ag-AgCl grounding wire to altered bath Cl^- levels. The error was approximately −6 mV and was determined by the shift in the measured zero-current potential upon superfusion with acetate solution prior to detection of modulation of the inward and outward current magnitudes.

The relative Na^+-to-K^+ permeability ratio (P_{Na}/P_K) was calculated from the shift in the reversal potential (E_{Na} and E_K) when the extracellular solution was changed from 149 Na^+/5 mM K^+ (E_{Na}) to 154 mM K^+ (E_K) in accordance with the following equation: $P_{Na}/P_K = (154\{\exp[F(E_{Na} - E_K)/RT]\} - 5)/149$, where 154 is the extracellular [K^+] (in mM) in the absence of Na^+, 149 and 5 are the extracellular [Na^+] and [K^+], respectively, (in mM) in the Na^+-containing solution, and R, T, and F are the standard physical constants.

When appropriate, data are presented as means ± SE. Statistical significance was determined using a Student's *t*-test for paired data or an analysis of variance, with the least significant difference determined by Bonferroni's multiple comparisons. Data are considered significant at $P \leq 0.05$.

All current records are of raw whole cell currents uncorrected for leakage currents. For clarity, brief uncompensated capacitative transients have been truncated in the presentation of currents recorded during voltage steps.

Western blotting

Protein extractions were performed in RIPA buffer (Sigma-Aldrich). Proteins were separated on an 8% SDS-polyacrylamide gel and transferred to a polyvinylidene difluoride membrane. The membrane was blocked for 1 h at room temperature in 5% milk in PBS containing 0.5% Tween 20 (PBST) and incubated overnight at 4°C with goat anti-TRPM7 (2 μg/ml; Ab729, Abcam) in 5% milk-PBST. After the membrane was washed, it was incubated for 1 h at room temperature with a horseradish peroxidase-conjugated rabbit anti-goat antibody (1:80,000 dilution; Sigma-Aldrich), and horseradish peroxidase activity was detected using Amersham ECL (GE Healthcare, Little Chalfont, UK).

Europe PMC Funders Author Manuscripts

RESULTS

Detection of a non-voltage-activated K^+ conductance in HEL cells

To define the basal currents in nonactivated HEL cells, cells were whole cell patch-clamped with a KCl-based patch internal solution containing 1 mM free Mg^{2+} (*solution 1* supplemented with 1 mM Mg^{2+}, see MATERIALS AND METHODS) and superfused with an extracellular solution containing 149 mM Na^+/5 mM K^+ (*solution 9*). This nominally Ca^{2+}-free extracellular solution contained 1 mM Mg^{2+} and was supplemented with 400 nM clotrimazole to ensure that the measured currents were not contaminated by a Ca^{2+}-activated K^+ conductance known to be present in HEL cells. Figure 1*A* shows a representative instantaneous current-voltage (*I-V*) relationship obtained from voltage ramps from −103 to +97 mV from a holding potential of −23 mV. These and all subsequently stated voltages are corrected for the junction potential errors noted in MATERIALS AND METHODS. In this extracellular solution, the cell exhibited a near-linear *I-V* relationship up to approximately +40 mV, consistent with a lack of expression of delayed rectifier-type voltage-activated K^+ current, as previously reported in HEL cells (18). However, the cell exhibited a reversal potential more negative than −50 mV, consistent with expression of a dominant K^+ conductance, given the ionic composition of the extracellular and pipette solutions (see MATERIALS AND METHODS). In agreement with this conclusion, changing the extracellular solution to one containing 154 mM K^+ (*solution 10*) resulted in the generation of an inward current displaying modest inward rectification and a shift in the reversal potential to ~0 mV, the equilibrium potential for K^+ (Fig. 1*A*).

A voltage-step protocol was used to more carefully investigate the time-dependent activation/inactivation characteristics and voltage dependence of this K^+ current. Figure 1, *B* and *C*, shows whole cell currents recorded in 154 mM extracellular K^+ solution (*solution 10*) from the same cell depicted in Fig. 1*A*. Currents elicited by voltage steps from −103 to +97 mV from holding potentials of −3 mV (Fig. 1*B*) or −83 mV (Fig. 1*C*) showed no time-dependent activation or inactivation. Figure 1*D* shows the whole cell *I-V* relationships derived from the results presented in Fig. 1, *B* and *C*. The current showed no voltage dependence and displayed modest inward rectification, consistent with the ramp data presented in Fig. 1*A*. The *I-V* relationships obtained from holding potentials of −3 and −83 mV were indistinguishable, indicating that no current inactivation occurs as a result of holding at depolarized potentials.

The mean increase in the inward current at −90 mV in response to changing the extracellular solution from 5 to 154 mM K^+ is shown in Fig. 2*A* for cells dialyzed with KCl-based internal solution containing 1 mM Mg^{2+} (*solution 1* supplemented with 1 mM Mg^{2+}). The magnitude of the inward current at −90 mV was −52.8 ± 12.6 pA in 149 Na^+/5 mM extracellular K^+ solution (*solution 9*) and significantly increased to −163.7 ± 33.0 pA when the extracellular solution was changed to 154 mM K^+ (*solution 10*; $P \leq 0.05$, $n = 39$). Figure 2*B* shows the whole cell currents in 5 and 154 mM extracellular K^+ solution in a representative experiment. These data clearly demonstrate a shift in the reversal potential toward 0 mV, the K^+ equilibrium potential when extracellular K^+ is elevated to 154 mM. The increase in K^+ current at negative potentials was not a result of anomalous permeability

arising from complete removal of extracellular Na^+, since a graded shift in the reversal potential and a graded increase in the magnitude of the inward current at −90 mV were observed in response to elevation of extracellular [K^+] from 5 to 73 or 154 mM (equimolar substitution of Na^+ for K^+; data not shown).

Constitutive expression of a Mg^{2+} inhibited TRPM7-like conductance

After transition to the whole cell configuration with a KCl-based pipette solution containing 1 mM Mg^{2+} (*solution 1* supplemented with 1 mM Mg^{2+}), an outwardly rectifying current at voltages greater than +40 mV was frequently observed. Such a current is clearly visible in the experiment presented in Fig. 2*B* and is present to a far lesser degree in Fig. 1*A*. This outwardly rectifying current was detected in 58 of 76 cells patched with a KCl-based internal solution supplemented with 1 mM free Mg^{2+} (*solution 1* supplemented with 1 mM Mg^{2+}). In 43 of the 58 cells, the outwardly rectifying current inactivated with variable kinetics. A representative experiment demonstrating the inactivation of this current is shown in Fig. 3, *A* and *B*. In this experiment, the cell was superfused with 149 Na^+/5 mM K^+ solution (*solution 9*) and whole cell-patched using a KCl-based internal solution containing 1 mM free Mg^{2+} (*solution 1* supplemented with 1 mM Mg^{2+}). Immediately upon gaining the whole cell configuration, ramps from −103 to +97 mV (Fig. 3*B*) were initiated every 3 s from a holding potential of −3 mV. The magnitude of the outward current at +90 mV, extracted from individual voltage ramps, is plotted as a function of time in Fig. 3*A* and demonstrates the time-dependent inactivation of this outward current. Representative instantaneous *I-V* relationships before and after current inactivation (Fig. 3*B*) reveal an outwardly rectifying current at potentials exceeding +40 mV. This inactivating outward current at potentials greater than +40 mV is reminiscent of TRPM7, a Mg^{2+}-inhibited current reported in a variety of cell types (20, 26, 33).

To confirm that the constitutively expressed outwardly rectifying current was Mg^{2+}-sensitive, experiments were performed using a nominally Mg^{2+}-free KCl-based internal solution (*solution 1*) to activate TRPM7 (20, 26, 33). The cell was superfused with 149 Na^+/5 mM K^+ saline solution (*solution 9*), and voltage ramps were applied every 3 s from a holding potential of −23 mV (Fig. 3*D*). The current at +90 mV was extracted from individual ramps and plotted as a function of time after attainment of the whole cell configuration in Fig. 3*C*. Dialysis with nominally Mg^{2+}-free KCl-based patch internal solution resulted in the time-dependent generation of an outward current at +90 mV. Representative instantaneous *I-V* relationships at different times during activation of this current are shown in Fig. 3*D*. The activation of an outward current at potentials greater than +40 mV when cells were dialyzed with a nominally Mg^{2+}-free patch solution and the partial inactivation of an indistinguishable constitutively expressed outward current when cells were dialyzed with 1 mM free Mg^{2+}-containing internal solution are consistent with modulation of the current in HEL cells by intracellular Mg^{2+}. Such a finding is consistent with the Mg^{2+} sensitivity of TRPM7 and other molecularly unidentified Mg^{2+}-inhibited cation (MIC) currents reported in a variety of cell types (20, 26, 33).

Experiments were undertaken to determine if the outwardly rectifying current displayed characteristics of TRPM7. When cells were dialyzed with a nominally Mg^{2+}-free, NMDG-

Cl-based internal solution (*solution 2*), the marked outward current in 149 mM Na^+/5 mM K^+ extracellular solution (*solution 9*) was absent, consistent with K^+ being the outward current-carrying ion (Fig. 4*A*; *n* = 3). Simultaneous reduction of intracellular (*solution 5*) and extracellular Cl^- (*solution 11*) solutions had no influence on generation of the outwardly rectifying current when the cell was dialyzed with the nominally Mg^{2+}-free low-Cl^--based K^+ internal solution (*solution 5*, *n* = 8; Fig. 4*B*). These data are consistent with little contribution of Cl^- to the outwardly rectifying current, further supporting the conclusion that K^+ is the outward current-carrying ion, as previously reported for TRPM7 (26).

The outward current activated by dialysis with nominally Mg^{2+}-free KCl internal solution (*solution 1*) was partially and reversibly blocked by 100 μM 2-APB, a feature of TRPM7-like currents in Jurkat cells (31) (Fig. 4*C*; *n* = 7 for block, *n* = 6 for reversibility of block). Additionally, the changes in the whole cell *I-V* relationship following superfusion with divalent-free extracellular solution (*solution 12*) were similar to those reported for TRPM7 and TRPM7-like currents in other cell types (19, 20, 26, 31). After dialysis with nominally Mg^{2+}-free KCl-based internal solution (*solution 1*), application of divalent-free extracellular solution resulted in loss of the marked outward rectification and an increase in inward current at negative potentials (Fig. 4*D*). These changes in the *I-V* relationship were fully reversible upon return to divalent-containing solution.

Finally, TRPM7 was immunodetected in Western blots using a commercially available antibody to human TRPM7. A prominent band at the correct molecular weight was detected in whole cell lysates from unactivated HEL cells (Fig. 5). A similar band was also detected in CHRF-288-11 cells, a leukemic cell line also devoid of voltage-activated K^+ channel activity (18) and also used as a model for megakaryocyte function.

Taken in concert, the outwardly rectifying *I-V* relationship in cells dialyzed with nominally Mg^{2+}-free internal solution, the suppression of this outward K^+ current by millimolar intracellular Mg^{2+}, the sensitivity of the current to 2-APB, the characteristic changes in the whole cell *I-V* relationship following removal of extracellular divalent ions, and the immunodetection of TRPM7 protein are consistent with the expression of a TRPM7 current in HEL cells with characteristics similar to those reported in other cell types (19, 20, 26, 31, 33). Importantly, the detection of the tell-tale outwardly rectifying current component of the *I-V* relationship at positive potentials immediately after the transition to the whole cell configuration with 1 mM Mg^{2+}-containing internal solution is consistent with constitutive activation of this current in the majority of HEL cells.

Non-voltage-activated K^+ current is a Mg^{2+}-inhibited K^+ current

Activation of the TRPM7 current during dialysis with nominally Mg^{2+}-free internal solution was frequently accompanied by a clear shift in the reversal potential to a more negative value, as evident in Fig. 3*D*. Such an observation is consistent with activation of a K^+ conductance, given the intra- and extracellular [K^+] and symmetrical Cl^- concentration used in these experiments. This K^+ conductance may arise from modulation of a Mg^{2+}-sensitive K^+ conductance during dialysis with nominally Mg^{2+}-free internal solution. Experiments were undertaken to define the sensitivity of the noninactivating, non-voltage-dependent K^+ current presented in Figs. 1 and 2 to changes in intracellular free [Mg^{2+}].

The magnitude of the inward current in HEL cells super-fused with 154 mM KCl-based extracellular solution (*solution 10*) was determined under conditions of 0 (nominally Mg^{2+}-free) and 5 mM free Mg^{2+} in the KCl-based patch internal solution (*solution 1*). Cells were first superfused with 149 Na^+/5 mM K^+ solution (*solution 9*) and dialyzed for ≥300 s to ensure complete activation or inactivation of the TRPM7 current. The extracellular solution was then changed to 154 mM K^+ (*solution 10*), and the magnitude of the inward current at −90 mV extracted from the voltage ramps administered every 3 s was determined. To remove the influence of variable levels of background currents, the "difference current" at −90 mV was calculated (current in 154 mM K^+ – current in 5 mM K^+). This difference current was normalized to cell capacitance to provide a measurement of current density and is presented as a function of free intracellular [Mg^{2+}] in Fig. 6*A*. For comparison, the difference current for experiments performed with 1 mM free Mg^{2+} (Fig. 2), normalized for cell capacitance, is included. The inward K^+ difference current measured with nominally Mg^{2+}-free internal solution (−38.5 ± 5.5 pA/pF) was significantly greater ($P \leq 0.05$) than that recorded in cells dialyzed with 1 mM free Mg^{2+} (−5.98 ± 1.1 pA/pF) and 5 mM free Mg^{2+} (−0.97 ± 0.2 pA/pF) solutions. As a result of this Mg^{2+} sensitivity, we have defined this current as a Mg^{2+}-inhibited K^+ (MIP) current.

The increase in MIP current was accompanied by a significant shift in the reversal potential measured in a 149 Na^+/5 mM K^+ solution (*solution 9*). The mean reversal potential for cells dialyzed with nominally Mg^{2+}-free internal solution (*solution 1*) or this internal solution supplemented with 1 or 5 mM free Mg^{2+} is shown in Fig. 6*B*. The reversal potential in cells dialyzed with nominally Mg^{2+}-free internal solution was −60.8 ± 2.5 mV ($n = 26$). In contrast, cells dialyzed with 1 mM free Mg^{2+} had a reversal potential of −32.5 ± 3.3 mV ($n = 39$), while cells dialyzed with 5 mM free Mg^{2+} had a reversal potential of −6.2 ± 6.5 mV ($n = 10$); all values are significantly different from each other ($P \leq 0.05$).

To quantify the changes in whole cell P_{Na} and P_K as a function of intracellular [Mg^{2+}], P_{Na} relative to P_K was estimated from the shift in the reversal potential when the extracellular solution was changed from 149 Na^+/5 mM K^+ (*solution 9*) to 154 mM K^+ (*solution 10*) in cells dialyzed with the three different free intracellular [Mg^{2+}] (*solution 1* supplemented with variable Mg^{2+}). The relative P_{Na}-to-P_K ratio (see MATERIALS AND METHODS) was 0.08 ± 0.01 ($n = 26$), 0.37 ± 0.04 ($n = 39$), and 0.66 ± 0.07 ($n = 10$) for nominally Mg^{2+}-free and 1 and 5 mM free internal Mg^{2+} solutions, respectively. All values are significantly different from each other ($P \leq 0.05$).

Inhibition of the MIP conductance may arise as a direct result of elevations in free cytosolic [Mg^{2+}]. Alternatively, inhibition may arise as a result of the formation of MgATP from endogenous ATP sources. Inhibition by MgATP must be considered, as MgATP has been demonstrated to inhibit the Mg^{2+}-sensitive TRPM7 currents (9). Experiments were undertaken to determine the role of MgATP in the modulation of the MIP conductance in HEL cells. Inclusion of 3 mM free ATP in the KCl-based patch internal solution in the absence of added Mg^{2+} (*solution 6*) still resulted in the detection of a robust MIP current not significantly different from that recorded in the absence of added ATP (−25.2 ± 6.2 pA/pF at −90 mV, $n = 5$). Therefore, elevation of free ATP in the absence of added Mg^{2+} has no significant effect on MIP current activation. To determine the role of MgATP in modulation

of the MIP conductance, cells were dialyzed with a pipette solution containing 3 mM free ATP and 5 mM MgATP (*solution 7*). The calculated free [Mg^{2+}] of this solution was 184 μM. A robust MIP current, indistinguishable from that recorded with 3 mM ATP alone, was also measured under these conditions (−25.3 ± 8.8 pA/pF at −90 mV, $n = 5$). Therefore, elevations in MgATP do not account for the suppression of the MIP current when Mg^{2+} is added to the pipette solution. In contrast, 5 mM free Mg^{2+} in the presence of 4.9 mM MgATP and a calculated free ATP concentration of 109 μM (*solution 8*) resulted in a significant suppression of the MIP current (−1.2 ± 0.4 pA/pF at −90 mV, $n = 6$, $P \leq 0.05$), consistent with inhibition arising from elevations in free [Mg^{2+}]. These data are summarized in Fig. 6*C*.

Pharmacology of the MIP and TRPM7 currents

Figure 7*A* shows the effect of extracellular Cs^+ on the inward MIP current recorded in 154 mM extracellular K^+ solution (*solution 10*) in a cell dialyzed with nominally Mg^{2+}-free internal solution (*solution 1*). Addition of 10 mM Cs^+ resulted in a reversible voltage-dependent block of the inward K^+ current. In 24 cells dialyzed with nominally Mg^{2+}-free internal solution, Cs^+ significantly reduced the K^+ difference current recorded at −90 mV to 14.4 ± 3.0% of control ($P \leq 0.05$; Fig. 7*D*) while having no effect on the outward TRPM7 current. An indistinguishable block was observed in cells dialyzed with 1 mM free Mg^{2+} (*solution 1* supplemented with 1 mM Mg^{2+}; 14.7 ± 3.3% of control, $n = 37$; Fig. 7*D*).

Extracellular Ba^{2+} (1 mM) also significantly blocked the inward K^+ current recorded in 154 mM K^+ (Fig. 7*A*), but to a lesser degree than 10 mM Cs^+. Ba^{2+} reversibly reduced the difference current in cells dialyzed with nominally Mg^{2+}-free internal solution (*solution 1*) to 43.5 ± 0.6% of control ($P \leq 0.05$, $n = 5$; Fig. 7*D*). The block by Ba^{2+} displayed evidence of voltage dependence (Fig. 7*A*). A thorough investigation of this phenomenon was not undertaken. The outward TRPM7 current was not blocked by this concentration of Ba^{2+}.

La^{3+} at 2 mM significantly blocked the inward K^+ current with a potency indistinguishable from 1 mM Ba^{2+} (Fig. 7*B*). La^{3+} reversibly reduced the difference current in cells dialyzed with nominally Mg^{2+}-free internal solution (*solution 1*) to 46.5 ± 5.6% of the control maximum ($P \leq 0.05$, $n = 9$, Fig. 7*D*). Unlike Ba^{2+} and Cs^+, La^{3+} also significantly reduced the outward TRPM7 current to 82.6 ± 1.7% of control ($P \leq 0.05$, $n = 9$; Fig. 7*B*). Block of the inward and outward currents was fully reversible.

In Fig. 4*C*, we demonstrated the inhibition by 2-APB of the outward TRPM7 current. 2-APB also blocked the inward MIP current. Figure 7*C* shows the effect of 100 μM 2-APB on a representative whole cell ramp *I-V* relationship recorded in 154 mM extracellular K^+ (*solution 10*) following dialysis with nominally Mg^{2+}-free internal solution (*solution 1*). In eight cells, 2-APB inhibited the inward K^+ difference current at −90 mV to 43.5 ± 9.2% of control. In the same cells, the whole cell current at +90 mV was simultaneously reduced to 31.1 ± 2.3% of control. Block of inward MIP and outward TRPM7 current was fully reversible; however, the time course of reversal was much longer than reversal of the block by Cs^+, Ba^{2+}, or La^{3+}.

The inward MIP and outward TRPM7 currents were unaffected by the ATP-sensitive K^+ (K_{ATP}) channel inhibitor glibenclamide (10 μM) and the hERG inhibitor E-4031 (2 μM; data not shown).

Isolation of the MIP current during TRPM7 activation using 5-lipoxygenase inhibitors

In an effort to dissociate TRPM7 from the MIP current, we investigated the effect of the 5-lipoxygenase inhibitors NDGA and AA-861 on our whole cell currents. Because both agents have been reported to inhibit TRPM7 (16), it may be possible to record the MIP current in the absence of TRPM7. A representative experiment is presented in Fig. 8. The cell was dialyzed with a Mg^{2+}-free KCl-based pipette internal solution containing 10 mM EGTA and 0.5 mM EDTA (*solution 3*), and ramps from −103 to +97 mV were administered every 3 s. The whole cell current at +90 and −90 mV was extracted from individual ramps and plotted as a function of time in Fig. 8*A*. TRPM7 activation as judged by the presence of a prominent outward current at potentials greater than +40 mV was accompanied by a negative reversal potential and significant outward current at 0 mV, consistent with the expression of the MIP current (*episode 152* in Fig. 8*B*). To confirm MIP current activation, the extracellular solution was changed from 149 Na^+/5 mM K^+ (*solution 9* without clotrimazole) to 154 mM KCl (*solution 10* without clotrimazole), resulting in the generation of the marked inward MIP current (*episode 163* in Fig. 8A). Application of 40 μM NDGA during high-K^+ application induced a surprising result. The inward MIP current was rapidly inhibited in the face of sustained outward TRPM7 current at positive potentials, thus allowing us to separate the MIP and TRPM7 currents. The *I-V* relationship after immediate inhibition of the MIP current looked very much like that expected for pure TRPM7 with little inward current. *I-V* relationships before and 6 s after application of NDGA (*episodes 163* and *167*, respectively) are shown in Fig. 8*B*. Subtraction of the *I-V* relationship immediately after rapid NDGA inhibition of the MIP current (*episode 167*) from that recorded before MIP current application (*episode 163*) yields the *I-V* relationship for the MIP conductance under conditions of high symmetrical K^+. This current is plotted as the difference current in Fig. 8*B*. The inwardly rectifying difference current (isolated MIP current) reversed at zero, the reversal potential for K^+, consistent with the MIP conductance being highly selective for K^+. The rapid inhibition of the inward MIP current was followed by a slow secondary inhibition of the residual outward TRPM7 current (Fig. 8, *A* and *C*). *Episode 197* demonstrates the secondary inhibition of the outward component of TRPM7. The full extent of the slow secondary inhibition of TRPM7 could not be studied, as prolonged exposure to NDGA resulted in loss of the seal and development of large leakage currents. NDGA inhibited the inward MIP current observed in high extracellular K^+ solution in five of five experiments.

Since NDGA enables us to separate the MIP and TRPM7 currents on the basis of temporally distinct inhibition of the two currents, experiments were performed in cells suspended in 145 Na^+/5 mM K^+ solution (*solution 9* without clotrimazole) to isolate the *I-V* relationship for pure MIP current under conditions of physiological [K^+]. A representative experiment is shown in Fig. 9. The cell was dialyzed with a Mg^{2+}-free KCl-based pipette internal solution containing 10 mM EGTA and 0.5 mM EDTA (*solution 3*), and ramps from −103 to +97 mV were administered every 3 s. We extracted the whole cell current at 0 and +90 mV and plotted these current magnitudes as a function of time in Fig. 9*A*. The current at 0 mV was

plotted, since pure TRPM7 reverses near zero. As a result, current recorded at this potential is attributable to the MIP current. The presence of a robust MIP current was first confirmed by exposure to 154 mM KCl-based solution (*solution 10* without clotrimazole). The currents during and after exposure to this high-K^+ solution (*episodes 229* and *243*, respectively; Fig. 9*B*, inset) demonstrate the presence of a robust MIP current. After return to 145 Na^+/5 mM K^+ solution, the whole cell *I-V* relationship showed the large outward TRPM7 current, a negative reversal potential, and significant outward current at 0 mV (*episode 243* in Fig. 9*B*). Exposure to 40 μM NDGA resulted in rapid complete inhibition of the MIP current recorded at 0 mV and a small inhibition of the outward current at +90 mV (Fig. 9*A*). The *I-V* relationship immediately after NDGA inhibition of the MIP current (Fig. 9*B*, *episode 252*) is indistinguishable from that expected for pure TRPM7. The *I-V* relationship displays little inward current, reverses close to 0 mV, and displays the outward rectification above +40 mV. Subtraction of the whole cell *I-V* relationship immediately after rapid NDGA inhibition of the MIP current, as judged by inhibition of the current at 0 mV (*episode 252* in Fig. 9, *A* and *B*) from that recorded before application (*episode 243* in Fig. 9, *A* and *B*), yields the *I-V* relationship for the MIP conductance under physiological conditions of intra- and extracellular [K^+]. This current is plotted as the difference current in Fig. 9*B*. The difference current (isolated MIP current) reversed at a negative potential close to the reversal potential for K^+, consistent with the MIP conductance being highly selective for K^+. Consistent with inhibition of the MIP current by NDGA, the magnitude of the inward current in 154 mM K^+ solution during NDGA application (*episode 271* in Fig. 9*B*, *inset*) was much less than that measured in its absence (*episode 229* in Fig. 9*B*, *inset*). NDGA rapidly inhibited the MIP current component of the whole cell *I-V* relationship in eight of eight experiments.

Continued exposure to NDGA resulted in a slow secondary inhibition of the pure TRPM7 current. Again, the full extent of this secondary inhibition of TRPM7 could not be determined, as NDGA resulted in loss of the seal and generation of large leakage currents.

We have also been able to isolate the MIP current by inhibition with the 5-lipoxygenase inhibitor AA-861 (15). A representative experiment is shown in Fig. 10. The cell was dialyzed with a Mg^{2+}-free KCl-based pipette internal solution containing 10 mM EGTA and 0.5 mM EDTA (*solution 3*), and ramps from −103 to +97 mV were applied every 3 s. The whole cell current at 0 and +90 mV was extracted from individual ramps and plotted as a function of time in Fig. 10*A*. The cell was briefly exposed to 154 mM K^+ solution (*solution 10* without clotrimazole) to confirm the presence of the MIP conductance. The *I-V* relationship during high-K^+ exposure is shown in Fig. 10*B*, *top inset* (*episode 163*). Return to 145 Na^+/5 mM K^+ (*solution 9* without clotrimazole) resulted in loss of the inward K^+ current, a negative reversal potential, and outward current at 0 mV, indicative of the MIP conductance (*episode 187* in Fig. 10*B*). Application of 40 μM AA-861 resulted in very rapid inhibition of the outward current at 0 mV and a small decline in the outward current at +90 mV. The *I-V* relationship immediately after inhibition of the current at 0 mV was indistinguishable from TRPM7, displaying a reversal potential much nearer 0 mV and the fingerprint outwardly rectifying current above +40 mV. The inhibited MIP current (difference current in Fig. 10*B*) determined by subtraction of the whole cell current immediately after AA-861 addition (*episode 196*) from that recorded in the absence of

AA-861 (*episode 187*) revealed an *I-V* relationship similar to that detected in Fig. 9 with use of NDGA. The difference current attributable to pure MIP current reversed at a very negative potential, indicative of selective K^+ permeability. Similar to NDGA, AA-861 also induced a slow secondary inhibition of the outward TRPM7 current recorded at +90 mV. However, AA-861 did not result in deterioration of the patch seal, allowing for determination of the extent of the TRPM7 inhibition and the extent of reversibility (Fig. 10*A*). Removal of AA-861 resulted in slow recovery of the outward current at 0 and +90 mV and a return to a highly negative reversal potential (*episode 326* in Fig. 10*B*, *bottom inset*). Exposure to high extracellular K^+ solution (*solution 10* without clotrimazole) after AA-861 washout resulted in the pronounced inward MIP current (*episode 308* in Fig. 10*B*, *bottom inset*) that is associated with the negative reversal potential in low-K^+ solution. AA-861 rapidly inhibited the MIP component of the whole cell *I-V* relationship in all seven experiments in which it was tested.

Taken in concert, NDGA and AA-861 rapidly inhibit the MIP current, the component of the whole cell current responsible for setting the negative reversal potential during dialysis with low intracellular Mg^{2+}.

Constitutive expression of the hyperpolarizing MIP conductance

Given the sensitivity of the magnitude of the MIP current to free intracellular [Mg^{2+}] (Fig. 6*A*) and the impact of this conductance on resting membrane potential (Fig. 6*B*), knowledge of the physiological relevance of this K^+ conductance is dependent on knowledge of the free [Mg^{2+}]. However, free [Mg^{2+}] is difficult to assess. If the declining outward TRPM7 current constitutively expressed in the majority of HEL cells (Fig. 3) arises as a result of Mg^{2+} inhibition of the current during whole cell dialysis, then a corresponding inhibition of the MIP conductance is predicted. Experiments were undertaken to investigate this hypothesis. Cells were suspended in 154 mM K^+ solution (*solution 10*) prior to transition to the whole cell configuration with a KCl-based pipette solution containing 5 mM free Mg^{2+} (*solution 1* supplemented with 5 mM Mg^{2+}). Immediately upon attainment of whole cell configuration, voltage ramps (Fig. 11*B*, *top*) were initiated every 3 s from a holding potential of −20 mV. The magnitude of the currents at +90 and −90 mV was extracted from each ramp and plotted as a function of time after transition to the whole cell configuration. The inward and the outward current components of the voltage ramp declined in a time-dependent fashion (Fig. 11*A*). In Fig. 11*B*, ramp *I-V* relationships immediately after attainment of whole cell mode and 531 s (episode 177) later are shown. The inward current in *episode 1* is indistinguishable from the MIP current, while the marked initial outward rectification at potentials greater than +40 mV is consistent with a TRPM7 conductance. Both currents inactivate, consistent with inhibition of both currents by 5 mM Mg^{2+} in the patch pipette solution (*solution 1* supplemented with 5 mM Mg^{2+}). An inactivating TRPM7 current was detected in 11 of 12 experiments in this series, with an inactivating inward MIP-like current clearly identified in 8 of these experiments. Therefore, MIP currents are constitutively active in the majority of HEL cells patched.

The time course of inactivation of the outward and inward currents was markedly different. The time course of inactivation of the TRPM7 and MIP currents in Fig. 11*A* is well fit by

double exponentials, yielding fast and slow time constants of 18 and 105.5 s, respectively, for inactivation of the outward TRPM7 current and 108.9 and 113.4 s, respectively, for inactivation of the inward MIP-like current. In the eight experiments where MIP-like current inactivation was observed, the fast time constant of inactivation of the outward TRPM7 conductance was 4.5 times faster than that of the inward MIP conductance [22.0 ± 3.1 s for TRPM7 current inactivation vs. 99.0 ± 19.6 s for MIP current ($P \leq 0.05$)]. These data further distinguish the MIP current from TRPM7.

It was necessary to ensure that the inward current detected in experiments such as those presented in Fig. 11, *A* and *B*, is, in fact, the MIP conductance. To address this issue, we used a protocol identical to that described for Fig. 11, *A* and *B*, to investigate the Cs^+ sensitivity of the MIP-like current. However, immediately after detecting the inward K^+ current following transition to the whole cell configuration, we changed the extracellular solution to a solution supplemented with 10 mM CsCl. In the experiment presented in Fig. 11*C*, this change was accompanied by marked inhibition of the inward current measured at −90 mV, consistent with the Cs^+ sensitivity of the MIP current. Ramp currents immediately before and after Cs^+ addition (Fig. 11*D*) reveal voltage-dependent block of the inward current contribution of the ramp. The blocking effect of Cs^+ was indistinguishable from its effect on the MIP current characterized earlier (Fig. 7). Washout of extracellular Cs^+ was accompanied by partial recovery of the inward current. The smaller inward current following Cs^+ removal is consistent with the inactivation of the constitutively expressed MIP current during continued dialysis with patch internal solution containing 5 mM free Mg^{2+} (*solution 1* supplemented with 5 mM Mg^{2+}). Replacement of 154 mM K^+ solution with 149 Na^+/5 mM K^+ resulted in a fall in the inward current at −90 mV, consistent with the K^+ sensitivity of this current. Further readdition of 10 mM CsCl resulted in inhibition of the small residual K^+ conductance observed in the presence of 5 mM intracellular Mg^{2+}. Cs^+ blocked the constitutively expressed inward current in seven of seven experiments, supporting the proposal that the MIP current underlies the inactivating current observed in Fig. 11, *A* and *B*.

MIP-like current expression in CHRF-288-11 cells

Experiments were undertaken to determine if expression of the MIP conductance is a more general feature of leukemic cells lacking voltage-activated K^+ channel function. Similar to HEL cells, CHRF-288-11 cells, a megakaryoblastic leukemic cell line, are devoid of voltage-activated K^+ channel function (18). In the nominal absence of intracellular Mg^{2+} following dialysis with KCl-based internal solution (*solution 1*), a MIP-like inward K^+ current was detected upon replacement of extracellular Na^+ with K^+ (*solution 10*; Fig. 12*A*). This inward current was blocked by Cs^+ in a voltage-dependent manner, consistent with the inhibition of MIP currents in HEL cells. The magnitude of the inward current in CHRF-288-11 cells was dependent on intracellular free [Mg^{2+}]. The magnitude of the K^+ difference current recorded at −90 mV was −7.6 ± 2.0 pA/pF in five cells dialyzed with nominally Mg^{2+}-free KCl-based internal solution (*solution 1*) and −0.7 ± 0.3 pA/pF in five cells dialyzed with 5 mM free Mg^{2+} solution ($P \leq 0.05$; Fig. 12*C*). In addition to the MIP current, cells dialyzed with nominally Mg^{2+}-free internal solution displayed an outwardly rectifying TRPM7-like current (Fig. 12, *A* and *B*). This outward current was absent when

cells were dialyzed with 5 mM Mg^{2+}-containing internal solution (data not shown). The Mg^{2+} sensitivity of the outwardly rectifying current, coupled with the immunodetection of TRPM7 in CHRF-288-11 cells (Fig. 5), supports the proposal that this current is most probably carried by TRPM7. Despite the coactivation of the TRPM7-like and MIP currents, the cells had a negative reversal potential when superfused with 149 Na^+/5 mM K^+ solution (*solution 9*). The reversal potential was −53.8 ± 5.3 mV in cells dialyzed with nominally Mg^{2+}-free internal solution and −22.8 ± 5.3 mV in cells dialyzed with 5 mM free Mg^{2+} solution ($P \leq 0.05$; Fig. 12*D*). Therefore, similar to HEL cells, MIP-like current activation in CHRF-288-11 cells is accompanied by hyperpolarization in the absence of a detectable voltage-gated K^+ conductance.

DISCUSSION

The present experiments confirm the absence of detectable voltage-gated K^+ currents in HEL cells (18). In its absence, we have detected constitutive activation of two Mg^{2+}-inhibited conductances. The first, the MIP current, is a novel Mg^{2+}-inhibited K^+ conductance that displayed no time-dependent activation or inactivation upon voltage steps but displayed inward rectification in symmetrical K^+ solution. The second is a Mg^{2+}-inhibited conductance displaying characteristics indistinguishable from the ubiquitously expressed TRPM7. Both currents were inhibited by the 5-lipoxygenase inhibitors NDGA and AA-861. However, because inhibition of the MIP current was much faster than inhibition of TRPM7, we were able to use subtraction of the whole cell currents before and shortly after addition of the inhibitors to isolate the MIP *I-V* relationship in the absence of TRPM7. In physiological [K^+] gradients, the isolated MIP current reversed at negative potentials close to the K^+ equilibrium potential, indicative of a highly selective P_K. While the isolated MIP current presented in Fig. 9 is quite small, larger MIP currents were isolated, and the magnitude of these currents was related to the magnitude of the inward K^+ current recorded in high extracellular K^+ solution (data not shown). The origin of the inhibition by 5-lipoxygenase inhibitors is unclear. NDGA and AA-861 inhibition of native and expressed TRPM7 in human embryonic kidney (HEK-293) cells is independent of 5-lipoxygenase activity (15). The role of 5-lipoxygenase in regulation of the MIP current remains to be elucidated.

As evident from the data presented in Fig. 6, MIP current expression induced by low intracellular [Mg^{2+}] resulted in a negative membrane potential, a finding that is accounted for by a significant increase in the measured whole cell P_K relative to P_{Na}. This marked shift in the membrane potential to negative values was observed despite the activation of the TRPM7 conductance, which has a reversal potential near zero as a result of its nonselective cation/divalent cation permeability (26, 33). In the absence of the MIP conductance, the constitutive expression of TRPM7 in HEL cells would result in a depolarized resting membrane potential, given the absence of conventional resting K^+ channel expression in these cells. Thus, the constitutive expression of the MIP current reported in Fig. 11 is expected to play a crucial role in the maintenance of a hyperpolarized resting potential during constitutive TRPM7 activation. Such a conclusion is borne out by the data presented in Figs. 9 and 10. Inhibition of the MIP current by NDGA or AA-861 was accompanied by a significant shift in the reversal potential toward 0 mV, the reversal potential for the

remaining TRPM7 conductance. Clearly, the MIP current is important in the setting of a negative membrane potential in the presence of constitutive expression of TRPM7 and the absence of expression of alternative conventional K^+ conductances. Expression of the MIP conductance was not confined to HEL cells. A MIP-like conductance that was blocked by extracellular Cs^+ in a voltage-dependent manner was also detected in CHRF-288-11 cells, another leukemic cell line devoid of voltage-activated K^+ channel function (18). Expression of the MIP-like current in CHRF-288-11 cells was also accompanied by membrane hyperpolarization, despite the expression of TRPM7-like currents (Fig. 12, *A* and *B*), consistent with the results in HEL cells. Therefore, the MIP current plays an important role in the maintenance of a hyperpolarized resting membrane potential in both cell types.

The MIP current and TRPM7-like current in HEL cells share numerous characteristics. *1*) The MIP and TRPM7 currents are modulated by free intracellular [Mg^{2+}]. The Mg^{2+} dependence of molecularly identified TRPM7 and TRPM7-like conductances is well established (11, 17, 19-21, 26, 31, 33), and the present experiments demonstrate the Mg^{2+} sensitivity of the MIP conductance in HEL and CHRF-288-11 cells. *2*) Both currents are partially and reversibly blocked by 2-APB, a feature shared with TRPM7 and TRPM7-like currents in other tissues (11, 13, 17, 22, 31). *3*) The MIP and TRPM7 currents are blocked by La^{3+}, although to a lesser degree than reported for TRPM7 channels in other cells (11, 17, 33). In the present experiments, 2 mM La^{3+} blocked the inward MIP current by ~53% and the outward MIC current by only ~18%. In contrast, millimolar La^{3+} has been reported to block the inward TRPM7 current by 97% (33) and outward TRPM7 currents by 37–82% (11, 17, 33). In addition, the TRPM7 and MIP currents display identical sensitivities to changes in intracellular pH, an established feature of TRPM7 currents in other cell types (21). Acidification induced by extracellular exposure to acetate markedly inhibited, in a reversible manner, both the inward K^+ current attributed to the MIP conductance when cells were suspended in high extracellular K^+ solution and the outward TRPM7 current at depolarized potentials (data not shown). Additionally, both currents were augmented by intracellular alkalinization induced by exposure to extracellular NH_4^+ (data not shown).

While both currents share similar characteristics, a major difference between the MIP and TRPM7 current in HEL cells is their sensitivity to the 5-lipoxygenase inhibitors NDGA and AA-861. While both currents were inhibited by these agents, the MIP conductance showed a much faster onset of inhibition, a characteristic that enabled us to isolate the MIP current from TRPM7. In addition, the two currents differ in their sensitivity to Ba^{2+}. While Ba^{2+} blocks the inward MIP current in HEL cells by ~56%, it has been reported to be ineffective as a blocker of inward and outward TRPM7 currents at the same concentration (33), distinguishing the inward MIP current from the inward current carried by heterologously expressed TRPM7.

The MIP conductance can also be distinguished from TRPM7 on the basis of the differing rates of inactivation of the endogenously activated currents (Fig. 11). During dialysis with 5 mM Mg^{2+} solution (*solution 1* supplemented with 5 mM Mg^{2+}), the outward TRPM7 current consistently inactivated with a fast inactivation time constant 4.5 times, on average, faster than the inward MIP current inactivation. Furthermore, in 3 of the 11 cells that displayed clear TRPM7 current inactivation, no MIP current inactivation was detected.

Despite modulation of both currents by intracellular Mg^{2+}, the ability to isolate the MIP current from TRPM7 using NDGA and AA-861, the sensitivity of the MIP current to extracellular Ba^{2+}, and the differential inactivation kinetics of MIP and TRPM7 conductances underlie our decision to refer to this as a MIP current, to distinguish it from TRPM7 channels.

Why has the MIP conductance not been reported in previous investigations of TRPM7? A simple answer may be that this conductance is unique to HEL and CHRF-288-11 cells, or leukemic cells in general. Alternatively, its detection in our experiments may arise from the experimental conditions. In the present experiments, we have studied an endogenous conductance, in contrast to previous reports studying cells heterologously overexpressing TRPM7 (26, 33). In addition, the present experiments were performed using K^+ as the outward current-carrying ion, instead of Cs^+, as used in numerous previous investigations of TRPM7 currents (2, 13, 19, 20, 22, 26, 33). Extracellular Cs^+ is frequently employed in investigations of TRPM7 to inhibit endogenous K^+ currents (13, 19, 21, 26, 33, 35). Our more physiological conditions could be used in HEL and CHRF-288-11 cells, given the absence of detectable conventional resting K^+ conductances and, hence, the lack of a requirement to inhibit such currents. Given the sensitivity of the MIP current to block by extracellular Cs^+, it is not surprising that MIP currents may have not been observed in past investigations of TRPM7 currents. The MIP conductance does not arise from the use in the present experiments of nominally Ca^{2+}-free extracellular solutions, as similar Mg^{2+}-dependent currents were observed in HEL cells in Ca^{2+}-containing solutions (data not shown).

While we could find no discussion of a Mg^{2+}-inhibited K^+ conductance in our search of the literature, we did find data consistent with such a conductance. During investigations of TRPM7 in rat microglia cells, Jiang and co-workers (17) performed experiments to determine the intracellular Mg^{2+} sensitivity of their TRPM7-like whole cell current. Pipette solutions devoid of added Mg^{2+} resulted in an increase in the TRPM7-like outward current and a shift in the reversal potential to more-negative values. Such a finding is identical to our findings in HEL cells. Given the ionic conditions in their experiments, the shift in reversal potential to more-negative values can be explained by an increase in the whole cell P_K, a conclusion consistent with our results. Interestingly, Jiang and co-workers also used intracellular K^+ as the outward current-carrying ion, and all extracellular solutions were devoid of Cs^+, conditions used in the present experiments. The origin of this increase in K^+ conductance in rat microglia cells is worthy of further investigation in the light of the present findings in HEL and CHRF-288-11 cells.

We have considered the possibility that low-level expression of a conventional K^+ conductance may underlie the MIP current in HEL cells. HEL cells express a robust Ca^{2+}-activated K^+ conductance (M. J. Mason, unpublished observations), making it necessary to rule out this conductance as the source of the hyperpolarizing influence observed in the absence of intracellular Mg^{2+}. The majority of the present experiments were performed in the nominal absence of extracellular Ca^{2+} and with internal solution containing 150 μM EGTA in the absence of added Ca^{2+}, conditions that do not support sustained activation of the Ca^{2+}-activated K^+ conductance in HEL cells (M. J. Mason, unpublished observations).

Additionally, extracellular solutions were supplemented with 200 or 400 nM clotrimazole, a potent inhibitor of the Ca^{2+}-activated K^+ current in HEL cells (M. J. Mason, unpublished observations). Furthermore, addition of clotrimazole after detection of the inward K^+ current had no effect, ruling out incomplete block of the Ca^{2+}-activated K^+ current as the source of the MIP current (data not shown). Finally, the isolation of the MIP current with NDGA and AA-861 was performed using a pipette internal solution containing 10 mM EGTA and 0.5 mM EDTA in the absence of added Ca^{2+} and Mg^{2+} (*solution 3*) and with extracellular solutions devoid of added Ca^{2+} (*solution 9* without clotrimazole). These solutions do not support activation of the Ca^{2+}-activated K^+ conductance in HEL cells. Under these conditions, an inward K^+ conductance was again observed in high extracellular K^+ solution. Taken in concert, these data rule out the endogenous Ca^{2+}-activated K^+ conductance as the source of the marked intracellular Mg^{2+}-sensitive inward K^+ current.

The inward rectification of the K^+ current in symmetrical K^+, its modulation by intracellular Mg^{2+}, and its sensitivity to extracellular Cs^+ and Ba^{2+} are characteristics of classical inwardly rectifying K^+ channels (16, 39, 40). According to the classical interpretation of Mg^{2+} modulation of inwardly rectifying K^+ channels, Mg^{2+}, in part, underlies inward rectification, by acting as a voltage-dependent channel pore blocker, resulting in inhibition of outward current flow (14, 16, 22, 37, 39). In contrast, in HEL cells, intracellular Mg^{2+} inhibits the inward current component of the *I-V* relationship when cells are superfused with high extracellular K^+ solution, rather than merely inhibiting outward current. The presence or absence of intracellular Mg^{2+} has no effect (40) or, at best, a marginal influence on the magnitude of the inward current component of the inward rectifier (IRK1) in rat basophilic leukemia (RBL) cells (M. J. Mason, unpublished observations), an observation at odds with the findings in the present experiments. Additionally, the inward component of the Mg^{2+}-sensitive K^+ current in HEL cells is reversibly inhibited by 2-APB. Preliminary experiments in RBL cells revealed little sensitivity of the inward rectifier to 2-APB (M. J. Mason, unpublished observations), again inconsistent with this channel underlying the Mg^{2+}-sensitive K^+ current in HEL cells. It would appear that the MIP conductance in HEL cells is distinct from classical inwardly rectifying K^+ currents.

The K_{ATP} channel inhibitor glibenclamide had no influence on the current, arguing against a role for these channels in the MIP current in HEL cells. In addition, the MIP current was detected when ATP and MgATP were included in the patch pipette, further evidence obviating a role for the K_{ATP} channel in the MIP conductance. The current was also unaffected by the selective hERG channel inhibitor E-4031. In addition, the current detected during negative voltage steps from −3 mV (Fig. 1*B*) did not reveal the time-dependent activation and inactivation expected of hERG (38). Furthermore, step currents recorded during voltage steps between −103 and −63 mV from a −3-mV holding potential were indistinguishable from those elicited from a holding potential of −83 mV (Fig. 1*D*), a voltage at which hERG channels are completely inactivated (38, 41), thus providing further evidence against a role for hERG in the MIP conductance.

The mechanism of inhibition by Mg^{2+} of the MIP current is unclear. The MIP current in HEL cells is not inhibited by 5 mM MgATP (Fig. 6*C*). Only when free [Mg^{2+}] was elevated is the MIP current inhibited. It has been proposed that Mg^{2+} and MgATP levels modulate

the TRPM7 current, possibly at two distinct sites (9, 19). It is interesting to note that, in addition to MIP currents, large outward TRPM7 currents were also consistently detected in the presence of 5 mM MgATP. In the presence of 5 mM MgATP, 184 μM free ATP, and 3 mM free ATP, the TRPM7-like current at +90 mV was 1,067.5 ± 547.6 pA (n = 5). This is not significantly different from 887.0 ± 82.0 pA (n = 5), which was recorded in cells dialyzed with patch internal solution supplemented with 3 mM free ATP in the absence of added Mg^{2+}, supporting the hypothesis that the TRPM7 conductance in HEL cells, similar to that in RBL-2H3 cells, is inhibited preferentially by free Mg^{2+} (19), rather than MgATP, as reported for cloned TRPM7 channels (9).

Phosphatidylinositol 4,5-bisphosphate (PIP_2) has been implicated in activation of TRPM7 channels (24). Mg^{2+}, polyvalent compounds, and intracellular protons have been proposed to inhibit TRPM7 activation via their ability to screen or bind to phosphates on PIP_2, effectively lowering its concentration near the channel (21). In addition to their modulation by intracellular free [Mg^{2+}], the MIP and TRPM7 currents in HEL cells are also augmented by intracellular alkalinization and inhibited by intracellular acidification, similar to MIC currents in RBL-2H3 cells and TRPM7 in recombinant expression systems (21). A requirement for PIP_2 binding may underlie the Mg^{2+} dependence and intracellular pH sensitivity of the MIP conductance if Mg^{2+} and protons function as PIP_2-screening agents, as proposed for TRPM7 currents (21). With this in mind, it is interesting to note that TASK-1, TASK-3, TREK-1, and TRAAK, members of the two-pore K^+ channel family of background K^+ currents, have been reported to be dependent on PIP_2 for activation (4, 5, 8, 23). MIP currents in HEL and CHRF-288-11 cells may arise from expression of PIP_2-dependent background two-pore K^+ channels. Further experiments are required to address this possibility.

The Mg^{2+} sensitivity of the MIP conductance in HEL cells raises the question of the physiological relevance of the current. Intracellular free [Mg^{2+}] has been reported to be 0.5–1 mM, well below the total Mg^{2+} content of mammalian cells (32). With 1 mM free Mg^{2+} in the patch pipette, a measurable K^+ current was detected in HEL cells, and this was accompanied by a negative reversal potential (Fig. 6). However, knowledge of the free [Mg^{2+}] in HEL cells is lacking; therefore, the level of activation of the MIP current in intact cells is uncertain. In an attempt to overcome this uncertainty, we have exploited the Mg^{2+} sensitivity of the outward TRPM7 current as a bioassay for free [Mg^{2+}] in the cell. In 58 of 76 HEL cells, an outwardly rectifying current at potentials greater than +40 mV was observed immediately upon gaining the whole cell configuration with 1 mM free Mg^{2+} in the patch pipette. Constitutive expression of TRPM7 currents has been previously reported in the majority of cells from the rat PAS T cell line and in a very small proportion of RBL-2H3 cells (19). In the present experiments, 43 of 58 cells displaying a TRPM7-like current at positive potentials showed some degree of inactivation of this current during dialysis with 1 mM free Mg^{2+}. The fact that 74% of the cells exhibited TRPM7 current inactivation may indicate that in vivo Mg^{2+} levels are <1 mM. Therefore, the magnitude of the MIP current in intact cells is predicted to be greater than that recorded following thorough dialysis with pipette solutions containing 1 mM free Mg^{2+}. Constitutive expression of the MIP conductance under physiological conditions of intracellular [Mg^{2+}] is supported

by the observation that inactivation of the constitutively expressed outward TRPM7 current during dialysis with 5 mM Mg^{2+} is paralleled by inactivation of the Cs^{+}-sensitive MIP current (Fig. 11).

The extent to which the MIP conductance is expressed in other cell types remains to be determined. Is it confined to the HEL and CHRF-288-11 cells, or could it be a more general conductance expressed in leukemia or other forms of cancers? Furthermore, the role of this conductance in malignant cell proliferation needs attention.

REFERENCES

1. Arcangeli A, Bianchi L, Becchetti A, Faravelli L, Coronello M, Mini E, Olivotto M, Wanke E. A novel inward-rectifying K^{+} current with a cell-cycle dependence governs the resting potential of mammalian neuroblastoma cells. J Physiol. 1995; 498:455–471. [PubMed: 8847640]
2. Bessac BF, Fleig A. TRPM7 channel is sensitive to osmotic gradients in human kidney cells. J Physiol. 2007; 582:1073–1086. [PubMed: 17510191]
3. Bianchi L, Wible B, Arcangeli A, Taglialatela M, Morra F, Castaldo P, Crociani O, Rosati B, Faravelli L, Olivotto M, Wanke E. *herg* encodes a K^{+} current highly conserved in tumors of different histogenesis: a selective advantage for cancer cells? Cancer Res. 1998; 58:815–822. [PubMed: 9485040]
4. Chemin J, Girard C, Duprat F, Lesage F, Romey G, Lazdunski M. Mechanisms underlying excitatory effects of group 1 metabotropic glutamate receptors via inhibition of 2P domain K^{+} channels. EMBO J. 2003; 22:5403–5411. [PubMed: 14532113]
5. Chemin J, Patel AJ, Duprat F, Luaritzen I, Lazdunski M, Honoré E. A phospholipid sensor controls mechanogating of the K^{+} channel TREK-1. EMBO J. 2005; 24:44–53. [PubMed: 15577940]
6. Cherubini A, Taddei GL, Crociani O, Paglierani M, Buccoliero AM, Fontana L, Noci I, Borri P, Giachi M, Becchetti A, Rossati B, Wanke E, Olivotto M, Arcangeli A. HERG potassium channels are more frequently expressed in human endometrial cancer as compared to non-cancerous endometrium. Br J Cancer. 2000; 83:1722–1729. [PubMed: 11104572]
7. Crociani O, Guasti L, Balzi M, Becchetti A, Wanke E, Olivotto M, Wymore RS, Arcangeli A. Cell cycle-dependent expression of HERG1 and HERG1B isoforms in tumor cells. J Biol Chem. 2003; 278:2947–2955. [PubMed: 12431979]
8. Czirják G, Petheo GL, Spät A, Enyedi P. Inhibition of TASK-1 potassium channel by phospholipase C. Am J Physiol Cell Physiol. 2001; 281:C700–C708. [PubMed: 11443069]
9. Demeuse P, Penner R, Fleig A. TRPM7 channel is regulated by magnesium nucleotides via its kinase domain. J Gen Physiol. 2006; 127:421–434. [PubMed: 16533898]
10. Faravelli L, Arcangeli A, Olivotto M, Wanke E. A HERG-like K^{+} channel in rat F-11 DRG cell line: pharmacological identification and biophysical characterisation. J Physiol. 1996; 496:13–23. [PubMed: 8910192]
11. Hanano T, Hara Y, Shi J, Morita H, Umebayashi C, Mori E, Sumimoto H, Ito Y, Mori Y, Inoue R. Involvement of TRPM7 in cell growth as a spontaneously activated Ca^{2+} entry pathway in human retinoblastoma cells. J Pharm Sci. 2004; 95:403–419.
12. Hemmerlein B, Weseloh RM, Mello de Queiroz F, Knötgen H, Sánchez A, Rubio ME, Martin S, Schliephacke T, Jenke M, Radzun HJ, Stühmer W, Pardo LA. Overexpression of Eag1 potassium channels in clinical tumours. Mol Cancer. 2006; 5:41. [PubMed: 17022810]
13. Hermosura MC, Monteilh-Zoller MK, Scharenberg AM, Penner R, Fleig A. Dissociation of the store-operated calcium current I_{CRAC} and the Mg-nucleotide-regulated metal ion current MagNuM. J Physiol. 2002; 539:445–458. [PubMed: 11882677]
14. Hibino H, Inanobe A, Furutani K, Murakami S, Findlay I, Kurachi Y. Inwardly rectifying potassium channels: their structure, function and physiological roles. Physiol Rev. 2010; 90:291–399. [PubMed: 20086079]

15. Hsiang-Chin C, Xie J, Zhang Z, Su L, Yue L, Runnels LW. Blockade of TRPM7 channel activity and cell death by inhibitors of 5-lipoxygenase. PLos One. 2010; 5:e11161–e11169. [PubMed: 20567598]
16. Horie M, Irisawa H, Noma A. Voltage-dependent magnesium block of adenosine-triphosphate-sensitive potassium channel in guinea-pig ventricular cells. J Physiol. 1987; 387:251–271. [PubMed: 2443681]
17. Jiang X, Newell EW, Schlicter LC. Regulation of a TRPM7-like current in rat brain microglia. J Biol Chem. 2003; 274:42867–42876. [PubMed: 12904301]
18. Kapural L, Feinstein MB, O'Rourke F, Fein A. Suppression of the delayed rectifier type of voltage gated K^+ outward current in megakaryocytes from patients with myelogenous leukemias. Blood. 1995; 86:1043–1055. [PubMed: 7620158]
19. Kozak JA, Cahalan MD. MIC channels are inhibited by internal divalent cations but not ATP. Biophys J. 2003; 84:922–927. [PubMed: 12547774]
20. Kozak JA, Kerschbaum HH, Cahalan MD. Distinct properties of CRAC and MIC channels in RBL cells. J Gen Physiol. 2002; 120:221–235. [PubMed: 12149283]
21. Kozak JA, Matsushita M, Nairn AC, Cahalan MD. Charge screening by internal pH and polyvalent cations as a mechanism for activation, inhibition, and rundown of TRPM7/MIC channels. J Gen Physiol. 2005; 126:499–514. [PubMed: 16260839]
22. Li M, Jiang J, Yue L. Functional characterization of homo- and heteromeric channel kinases TRPM6 and TRPM7. J Gen Physiol. 2006; 127:525–537. [PubMed: 16636202]
23. Lopes CMB, Rohács T, Czirják G, Balla T, Enyedi P, Logothetis DE. PIP_2 hydrolysis underlies agonist-induced inhibition and regulates voltage gating of two-pore domain K^+ channels. J Physiol. 2005; 564:117–129. [PubMed: 15677683]
24. Matsuda H, Saigusa A, Irisawa H. Ohmic conductance through the inwardly rectifying K channel and blocking by internal Mg^{2+} Nature. 1987; 325:156–159. [PubMed: 2433601]
25. Mello de Queiroz F, Suarez-Kurtz G, Stühmer W, Pardo LA. Ether à go-go potassium channel expression in soft tissue sarcoma patients. Mol Cancer. 2006; 5:42. [PubMed: 17022811]
26. Nadler MJS, Hermosura MC, Inabe K, Perraud AL, Zhu Q, Stokes J, Kusosaki T, Kinet JP, Penner R, Scharenberg AM, Fleig AF. LTRPC7 is a Mg ATP-regulated divalent cation channel required for cell viability. Nature. 2001; 411:590–597. [PubMed: 11385574]
27. Neher E. Correction for liquid junction potentials in patch clamp experiments. Methods Enzymol. 1992; 207:123–131. [PubMed: 1528115]
28. Ng B, Barry PH. The measurement of ionic conductivities and mobilities of certain less common organic ions needed for junction potential corrections in electrophysiology. J Neurosci Methods. 1995; 56:37–41. [PubMed: 7715244]
29. Pardo LA, del Camino D, Sanchez A, Alves F, Bruggemann A, Beckh S, Stuhmer W. Oncogenic potential of EAG K^+ channels. EMBO J. 1999; 18:5540–5547. [PubMed: 10523298]
30. Pillozi S, Brizzi MF, Balzi M, Crociani O, Cherubini A, Guasti B, Bartolozzi B, Wanke E, Bernabei PA, Olivotto M, Pegoraro LY, Arcangeli A. HERG potassium channels are constitutively expressed in primary human acute myeloid leukemias and regulate cell proliferation of normal and leukemic hemopoietic progenitors. Leukemia. 2002; 16:1791–1798. [PubMed: 12200695]
31. Prakriya M, Lewis RS. Separation and characterisation of currents through store-operated CRAC channels and Mg^{2+}-inhibited cation (MIC) channels. J Gen Physiol. 2002; 119:487–508. [PubMed: 11981025]
32. Romani AM, Scarpa A. Regulation of cellular magnesium. Front Biosci. 2000; 5:D720–D734. [PubMed: 10922296]
33. Runnels LW, Yue L, Clapham DE. TRP-PLIK, a bifunctional protein with kinase and ion channel activities. Science. 2001; 291:1043–1047. [PubMed: 11161216]
34. Runnels LW, Yue L, Clapham DE. The TRPM7 channel is inactivated by PIP_2 hydrolysis. Nat Cell Biol. 2002; 4:329–336. [PubMed: 11941371]
35. Schmitz C, Perraud AL, Johnson CO, Inabe K, Smith M, Penner R, Kurosaki T, Fleig A, Scharenberg AM. Regulation of vertebrate cellular Mg^{2+} homeostasis by TRPM7. Cell. 2003; 114:191–200. [PubMed: 12887921]

36. Smith GA, Tsui HW, Newell EW, Jiang X, Zhu XP, Tsui FWL, Schlicter LC. Functional up-regulation of HERG K^+ channels in neo-plastic hematopoietic cells. J Biol Chem. 2002; 277:18528–18534. [PubMed: 11893742]

37. Stanfield PR, Davies NW, Shelton PA, Khan IA, Brammar WJ, Standen NB, Conley EC. The intrinsic gating of inward rectifier K^+ channels expressed from the murine IRK1 gene depends on voltage, K^+ and Mg^{2+} J Physiol. 1994; 475:1–7. [PubMed: 8189383]

38. Trudeau C, Warmke JW, Genetzky B, Robertson GA. HERG, a human inward rectifier in the voltage-gated potassium channel family. Science. 1995; 269:92–95. [PubMed: 7604285]

39. Vandenberg C. Inward rectification of a potassium channel in cardiac ventricluar cells depends on internal magnesium ions. Proc Natl Acad Sci USA. 1987; 84:2560–2564. [PubMed: 2436236]

40. Wischmeyer E, Lentes KU, Karschin A. Physiological and molecular characterization of an IRK-type inward rectifier K^+ channel in a tumour mast cell line. Pflügers Arch. 1995; 429:809–819. [PubMed: 7603835]

41. Zhou W, Cayabyab FS, Pennefather PS, Schlicter LC, DeCoursey TE. HERG-like K^+ channels in microglia. J Gen Physiol. 1998; 111:781–794. [PubMed: 9607936]

Europe PMC Funders Author Manuscripts

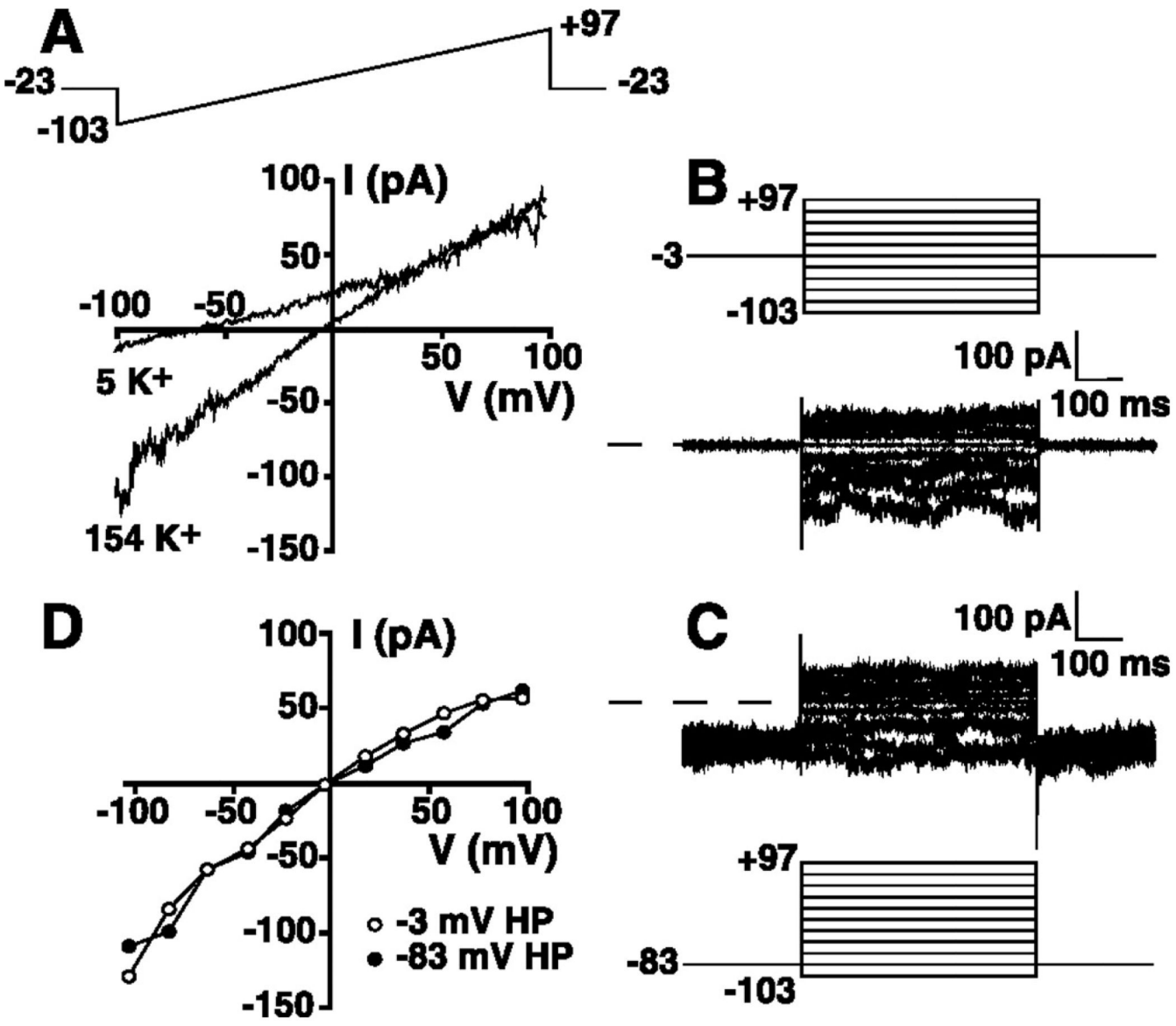

Fig. 1.

Detection of a non-voltage-activated, noninactivating K^+ conductance in human erythroleukemia (HEL) cells. *A*: whole cell current-voltage (*I-V*) relationship derived from voltage ramps in 149 Na^+/5 mM K^+ solution (*solution 9*) or 154 mM K^+ extracellular solution (*solution 10*). Cell was whole cell patch-clamped using a 154 mM KCl-based pipette solution (*solution 1*) supplemented with 1 mM Mg^{2+}, and the 200-ms voltage ramp (*top*) was administered every 3 s from a holding potential of −23 mV (these and all subsequent voltages are corrected for junction potential errors; see MATERIALS AND METHODS). *B*: whole cell currents recorded in 154 mM extracellular K^+ solution (*solution 10*) using a voltage-step protocol (*top*) from a holding potential of −3 mV. Voltage-step protocol consisted of 500-ms steps from −103 to +97 mV in 20-mV increments. *C*: whole cell currents recorded in 154 mM extracellular K^+ solution using a voltage-step protocol (*bottom*) from a holding potential of −83 mV. Voltage steps are identical to those

administered in *B*. *D*: *I*-*V* relationships for mean step currents recorded during voltage steps from holding potential of −3 mV (*B*) or −83 mV (*C*).

Europe PMC Funders Author Manuscripts

Europe PMC Funders Author Manuscripts

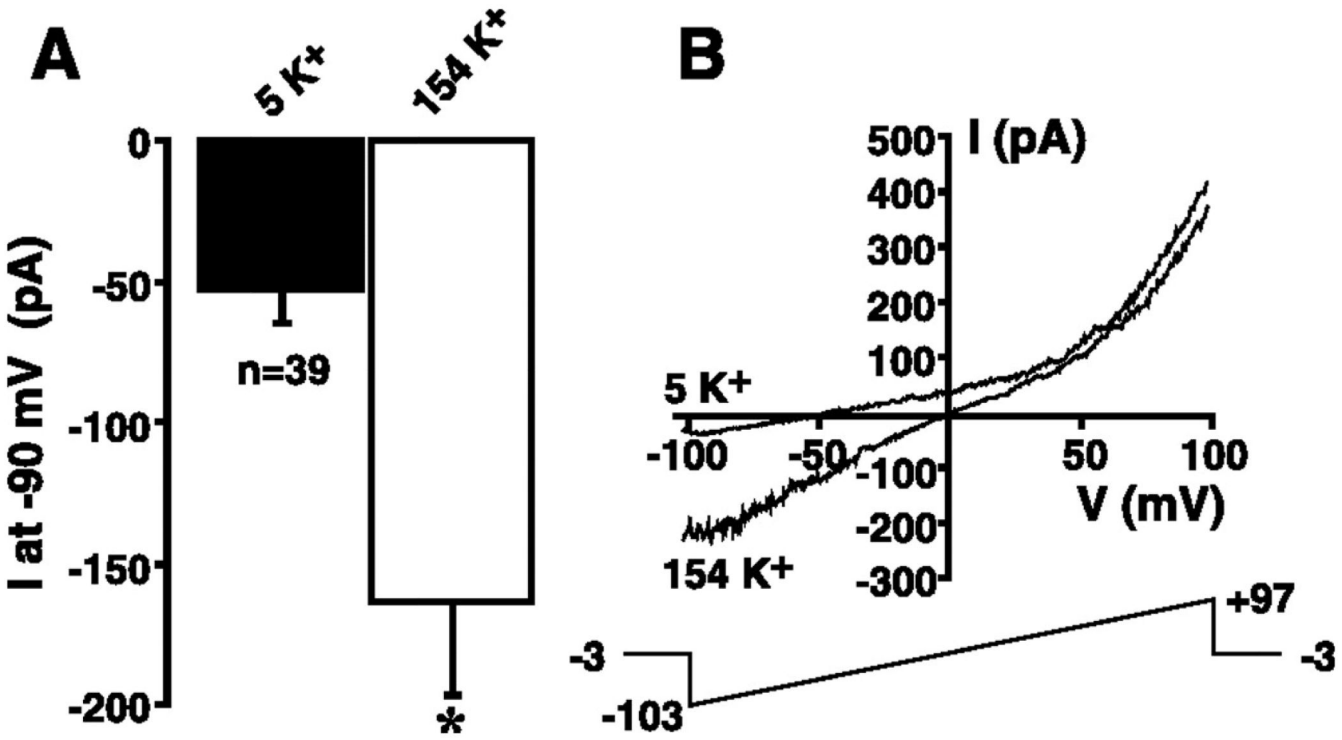

Fig. 2.

K^+ sensitivity of non-voltage-activated, noninactivating inward current in HEL cells. *A*: cells were whole cell patch-clamped using a KCl-based internal solution (*solution 1*) supplemented with 1 mM Mg^{2+}. Magnitude of the inward current recorded at −90 mV was extracted from 200-ms voltage ramps administered every 3 s in the presence 149 Na^+/5 mM K^+ solution (*solution 9*) or 154 mM K^+ extracellular solution (*solution 10*) under steady-state conditions. Voltage-ramp protocol is shown in *B*. *$P \leq 0.05$. *B*: cell was whole cell patch-clamped with a KCl-based internal solution (*solution 1*) supplemented with 1 mM Mg^{2+}. The 200-ms voltage ramp (*bottom*) was administered every 3 s during superfusion with 5 and 154 mM K^+ solutions.

Europe PMC Funders Author Manuscripts

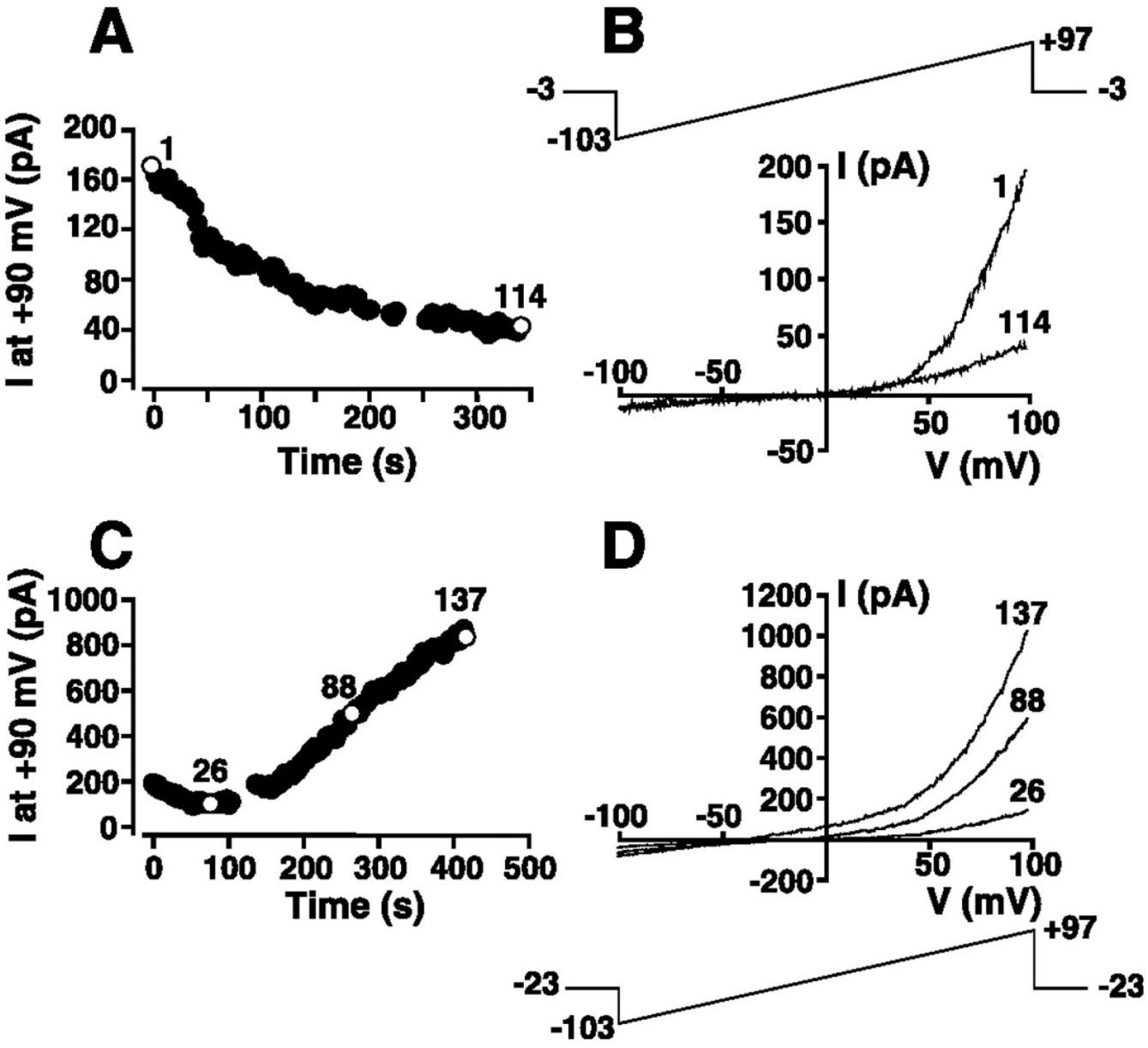

Fig. 3.

Modulation by intracellular free Mg^{2+} concentration ($[Mg^{2+}]$) of the outward component of the whole cell *I-V* relationship in HEL cells. *A*: cell suspended in 149 Na^+/5 mM K^+ solution (*solution 9*) was whole cell patch-clamped with a KCl-based internal solution (*solution 1*) supplemented with 1 mM Mg^{2+}. The 200-ms voltage-ramp protocol administered every 3 s is shown in *B*. Magnitude of the outward current at +90 mV was extracted from ramp data and plotted as a function of time. *B*: *I-V* relationships immediately after whole cell configuration was attained (*episode 1*) and 339 s later (*episode 114*) in experiment presented in *A*. *C*: cell was whole cell patch-clamped with a nominally Mg^{2+}-free KCl-based internal solution (*solution 1*). The 200-ms voltage-ramp protocol is shown in *D*. Magnitude of the outward current at +90 mV was extracted from ramp data and plotted as a function of time.

D: *I-V* relationships corresponding to *episodes 26*, *88*, and *137* after whole cell configuration was attained in experiment presented in *C*.

Europe PMC Funders Author Manuscripts

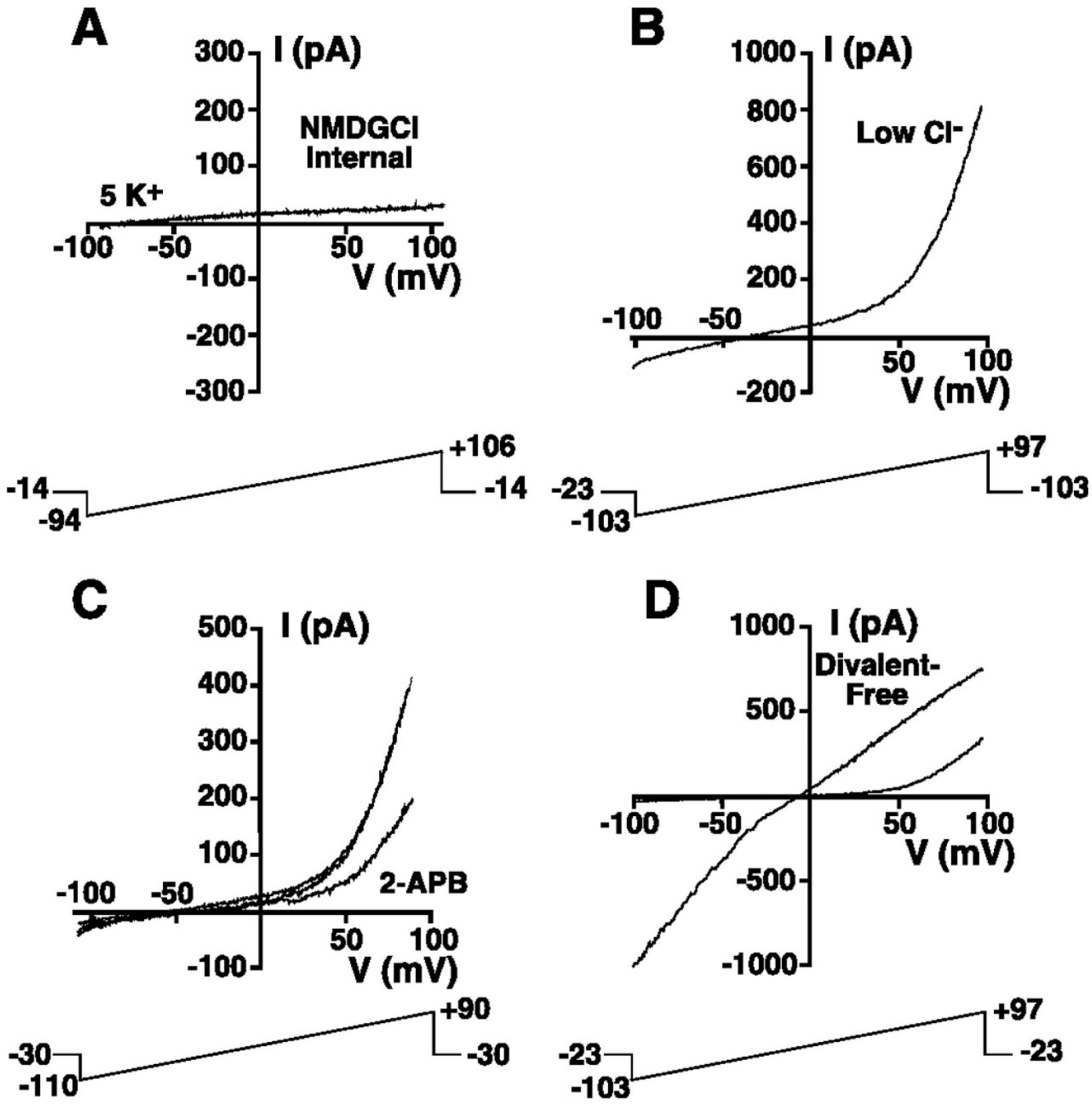

Fig. 4.

Characterization of a TRPM7-like current in HEL cells. *A*: representative whole cell ramp current recorded in a cell suspended in 149 Na^+/5 mM K^+ solution (*solution 9*) and whole cell patch-clamped using nominally Mg^{2+}-free, NMDG-Cl-based internal solution (*solution 2*). The 200-ms voltage ramps were administered every 3 s. *B*: representative whole cell ramp current recorded in low intra- and extracellular Cl^- solutions. Cell was suspended in Na^+-methanesulfonate solution containing 2 mM Cl^- (*solution 11*) and whole cell patch-clamped with a nominally Mg^{2+}-free, K^+-glutamate-based internal solution containing 2

mM Cl^- (*solution 5*). The 200-ms voltage ramps were administered every 3 s. *C*: representative ramp currents before, during, and after exposure to 100 μM 2-aminoethoxydiphenyl borate (2-APB). Cell was whole cell patch-clamped with a nominally Mg^{2+}-free, K^+-glutamate internal solution identical to that used in *B* (*solution 5*) and superfused with 149 Na^+/5 mM K^+ solution (*solution 9*) in the presence and absence of 100 μM 2-APB. The 200-ms voltage ramps were administered every 3 s. *D*: whole cell ramp currents recorded in the presence and absence of extracellular divalent ions. Cell was whole cell patch-clamped with a nominally Mg^{2+}-free KCl-based internal (*solution 1*) in the presence (145 Na^+/5 mM K^+; *solution 9*) and absence (145 Na^+/5 mM K^+ solution devoid of added divalent ions and supplemented with 10 mM *N*-2-hydroxyethyl-EDTA; *solution 12*) of extracellular divalent ions. The 200-ms voltage ramp was administered every 1 s.

Europe PMC Funders Author Manuscripts

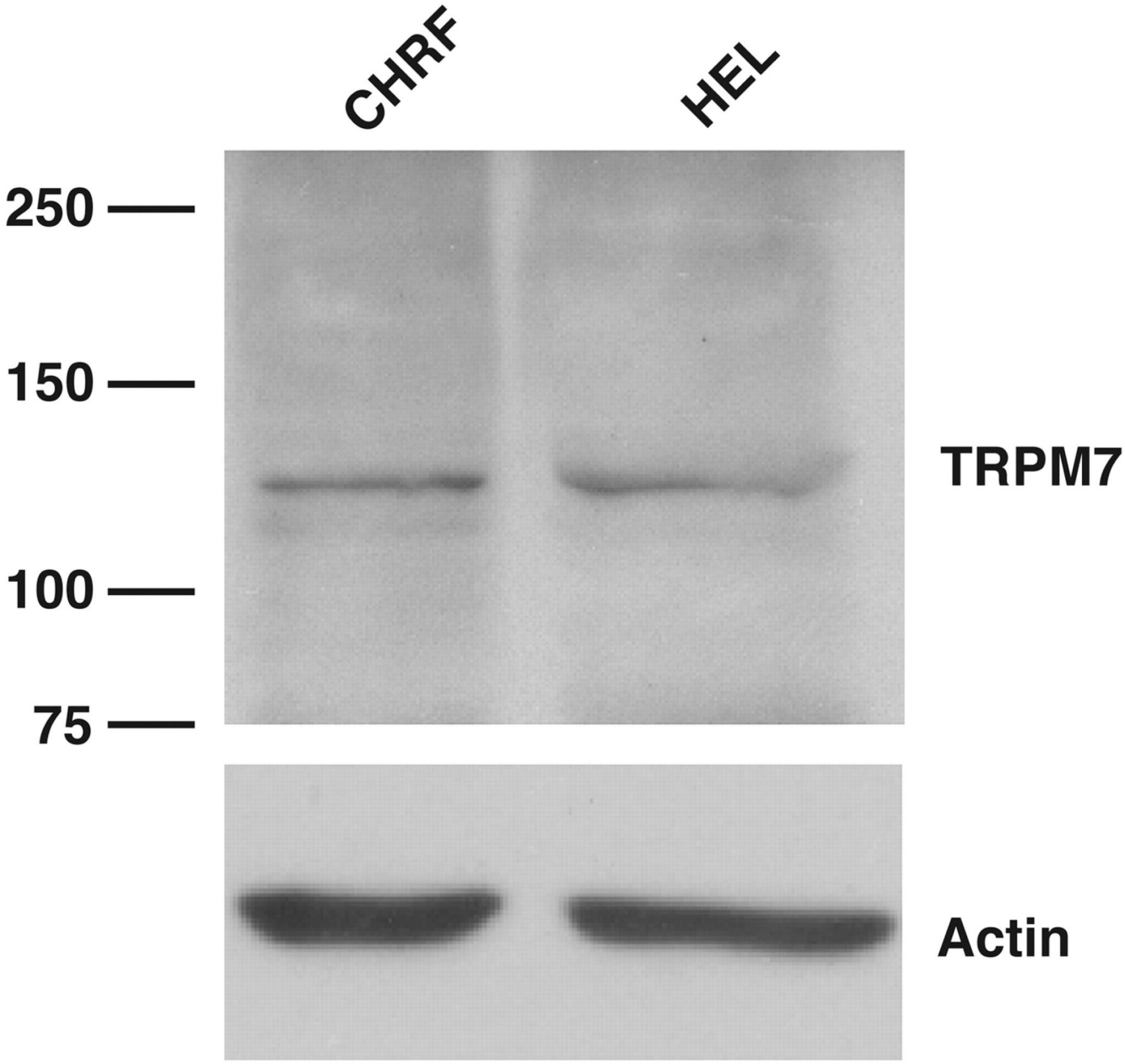

Fig. 5.

Immunodetection of TRPM7 in HEL and CHRF-288-11 cells. Protein extracts were prepared and immunoblotted. A commercially available TRPM7 antibody (Ab729, Abcam) was used to detect bands at the appropriate molecular mass (*left*) in CHRF-288-11 (CHRF) and HEL cells. Immunodetection of actin is shown for control of protein loading.

Europe PMC Funders Author Manuscripts

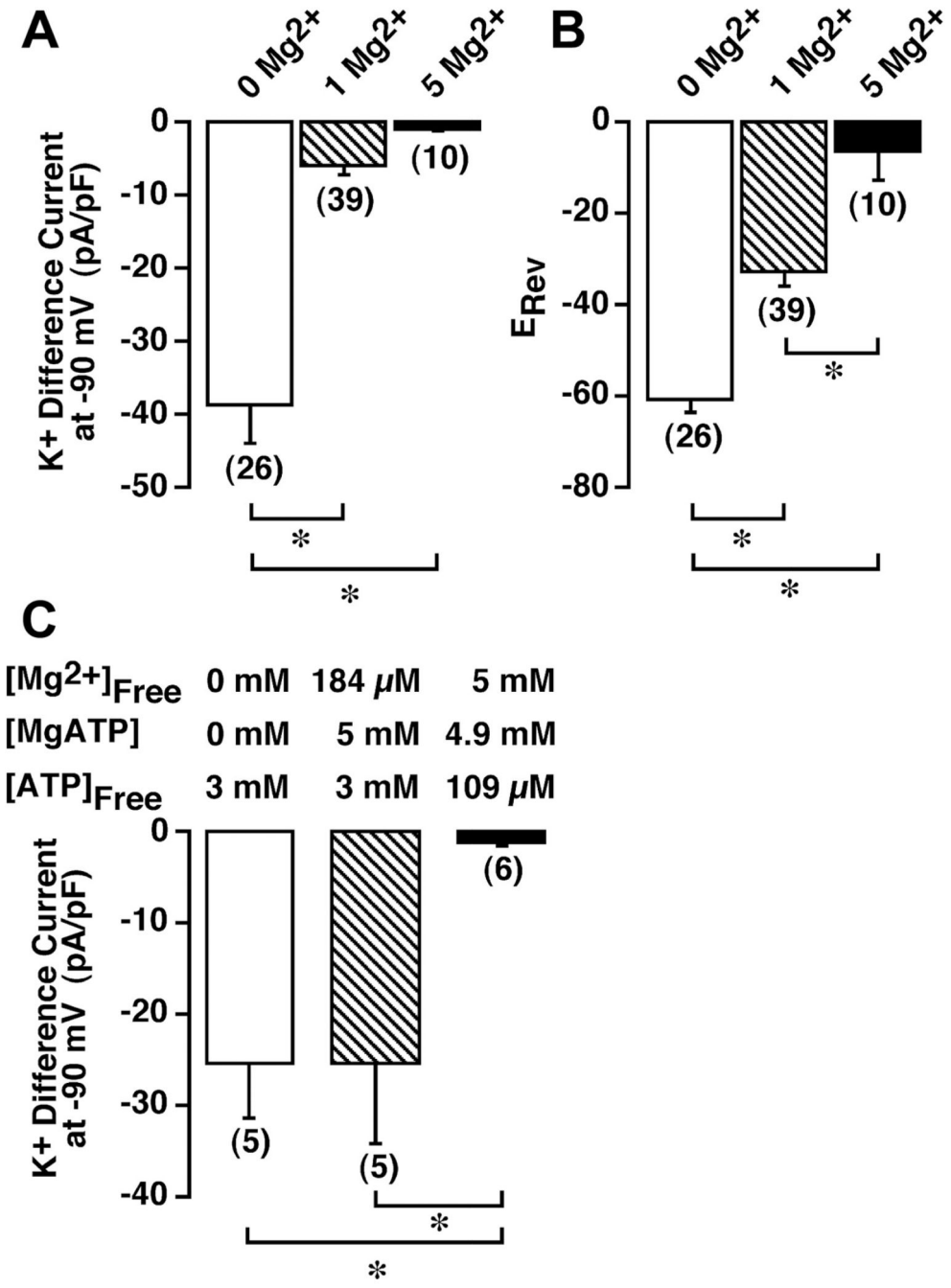

Fig. 6.

Sensitivity of inward K^+ current to inhibition by free intracellular Mg^{2+} and MgATP concentrations in HEL cells. *A*: cells were whole cell patch-clamped with a KCl-based internal solution (*solution 1*) that was nominally Mg^{2+}-free (0 Mg^{2+}) or contained 1 or 5 mM free Mg^{2+}, and 200-ms voltage ramps from −103 to +97 mV were administered every 3 s from a holding potential of −3 mV. Cells were dialyzed for ≥300 s, and the K^+ difference current was calculated as the magnitude of the current at −90 mV in 154 mM K^+ solution (*solution 10*) minus the magnitude of the current at the same potential in 149 Na^+/5 mM K^+

solution (*solution 9*). Currents were normalized to cell capacitance. *B*: reversal potential (E_{Rev}) averaged over 5 consecutive ramps was determined in 149 Na^+/5 mM K^+ solution. *C*: magnitude of the K^+ difference current at −90 mV under different conditions of free Mg^{2+} and MgATP (*solutions 6–8*). Numbers in parentheses denote sample size. **P* ≤ 0.05.

Europe PMC Funders Author Manuscripts

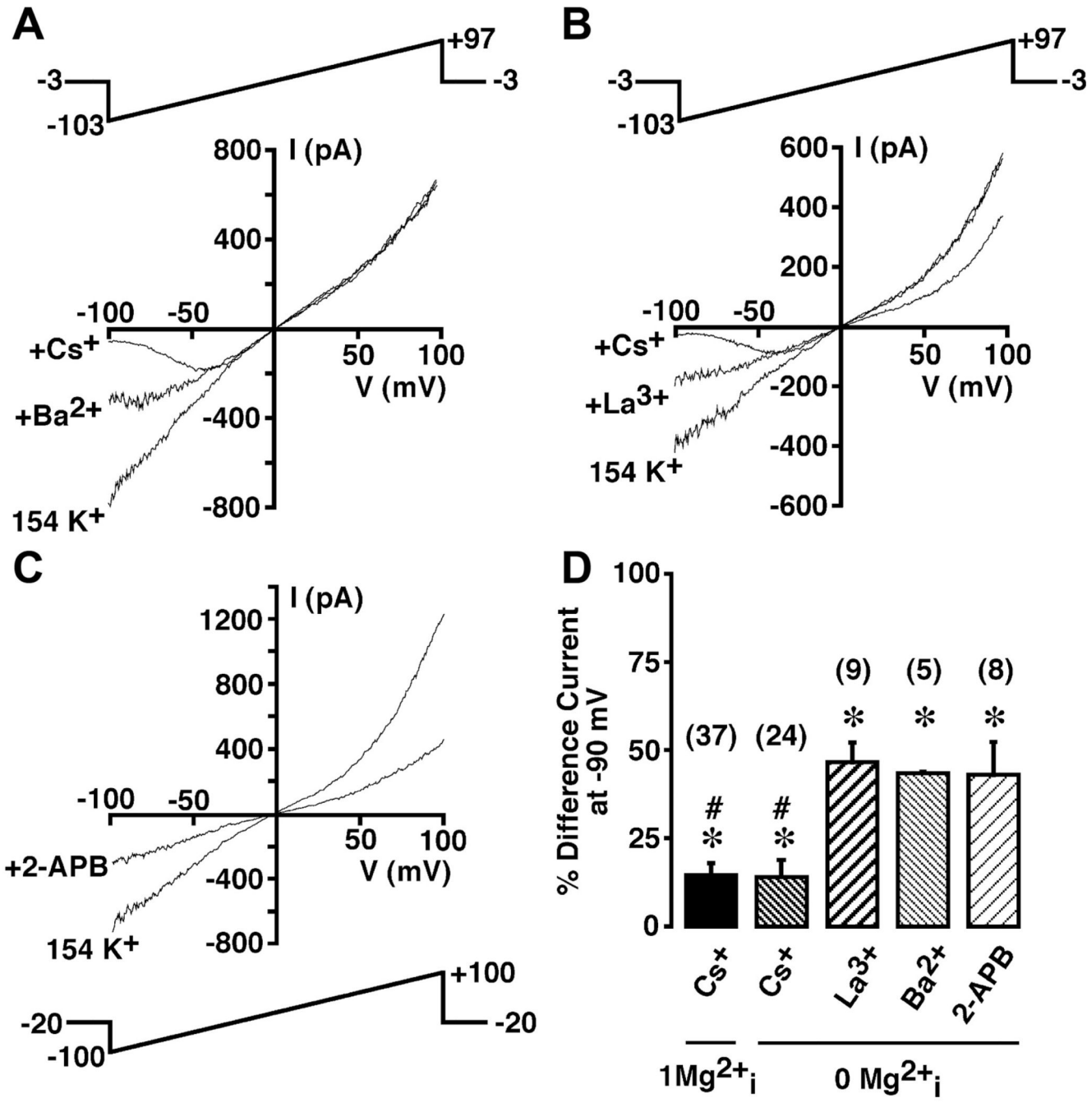

Fig. 7.

Sensitivity of Mg^{2+}-inhibited K^+ (MIP) and TRPM7 current to Cs^+, Ba^{2+}, La^{3+}, and 2-APB in HEL cells. *A*: cell was superfused with 154 mM K^+ solution (*solution 10*) during whole cell patch clamp with a nominally Mg^{2+}-free KCl-based internal solution (*solution 1*). The 200-ms voltage ramp (*top*) was administered every 3 s in the presence and absence of 10 mM Cs^+ and 1 mM Ba^{2+}, and whole cell *I-V* relationships were plotted. *B*: whole cell *I-V* relationships under conditions identical to those described in *A* in the presence and absence of 10 mM Cs^+ and 2 mM La^{3+}. *C*: whole cell *I-V* relationships under conditions identical to

those described in *A* in the presence and absence of 100 μM 2-APB. Holding potential was −20 mV. *D*: summary of inhibitory influence of Cs^+, Ba^{2+}, La^{3+}, and 2-APB. Data are presented as percentage of control K^+ difference current remaining in the presence of 10 mM Cs^+, 1 mM Ba^{2+}, 2 mM La^{3+}, and 100 μM 2-APB. Numbers in parentheses denote sample size. Mg_i^{2+}, intracellular Mg^{2+}. *$P \leq 0.05$ vs. control. #$P \leq 0.05$ vs. La^{3+}, Ba^{2+}, and 2-APB.

Europe PMC Funders Author Manuscripts

Europe PMC Funders Author Manuscripts

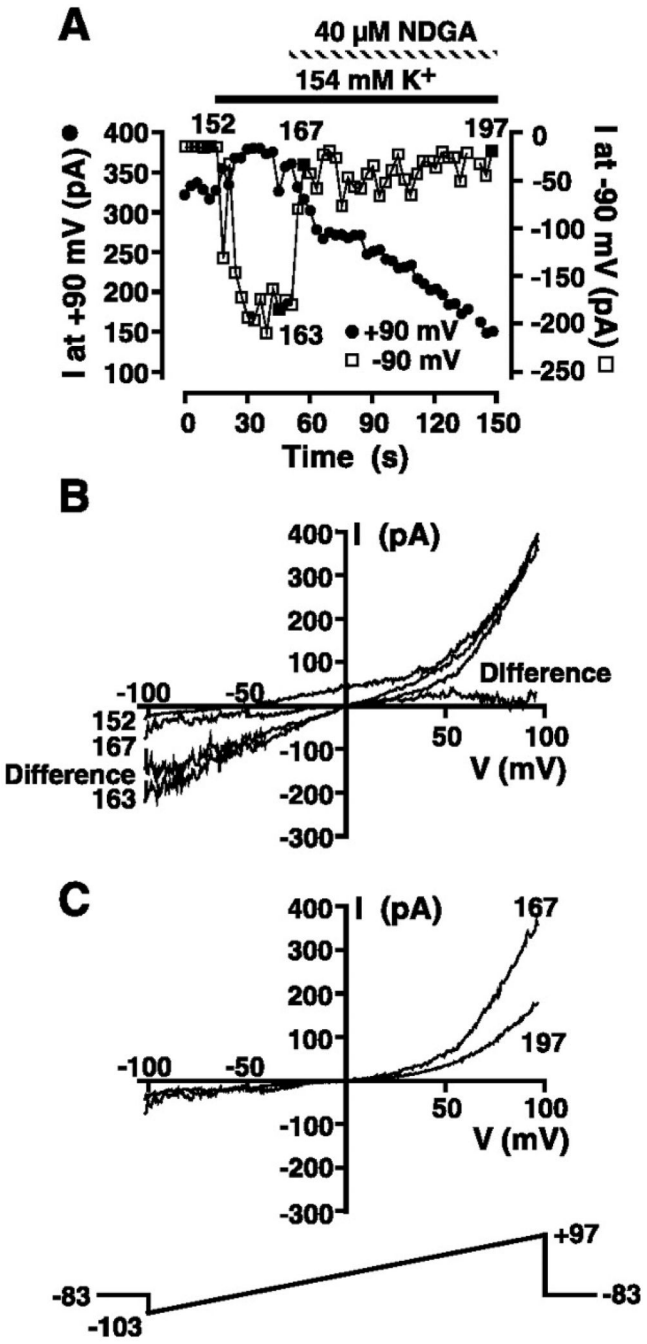

Fig. 8.

Inhibition by nordihydroguaiaretic acid (NDGA) of MIP current recorded in high extracellular K^+ solution. *A*: cell suspended in 149 Na^+/5 mM K^+ solution (*solution 9*) was whole cell patch-clamped with a Mg^{2+}-free KCl-based internal solution (*solution 3*). The 200-ms voltage-ramp protocol administered every 3 s is shown in *C*. Magnitude of the outward current at +90 and −90 mV was extracted from ramp data and plotted as a function of time. Where indicated, extracellular solution was changed to 154 mM K^+ (*solution 10*) and 40 μM NDGA was applied. *B*: *I-V* relationships in 149 Na^+/5 mM K^+ solution (*solution*

9; *episode 152*), 154 mM K^+ (*solution 10*; *episode 163*), and immediately after (*episode 167*) application of NDGA. *I-V* relationship labeled "Difference" was obtained by subtraction of *I-V* relationship after NDGA addition (*episode 167*) from that before (*episode 163*) application of NDGA and is the *I-V* relationship for MIP conductance in the absence of TRPM7 contamination. *C*: *I-V* relationships corresponding to *episodes 167* and *197* in the sustained presence of 40 μM NDGA as denoted in *A*.

Europe PMC Funders Author Manuscripts

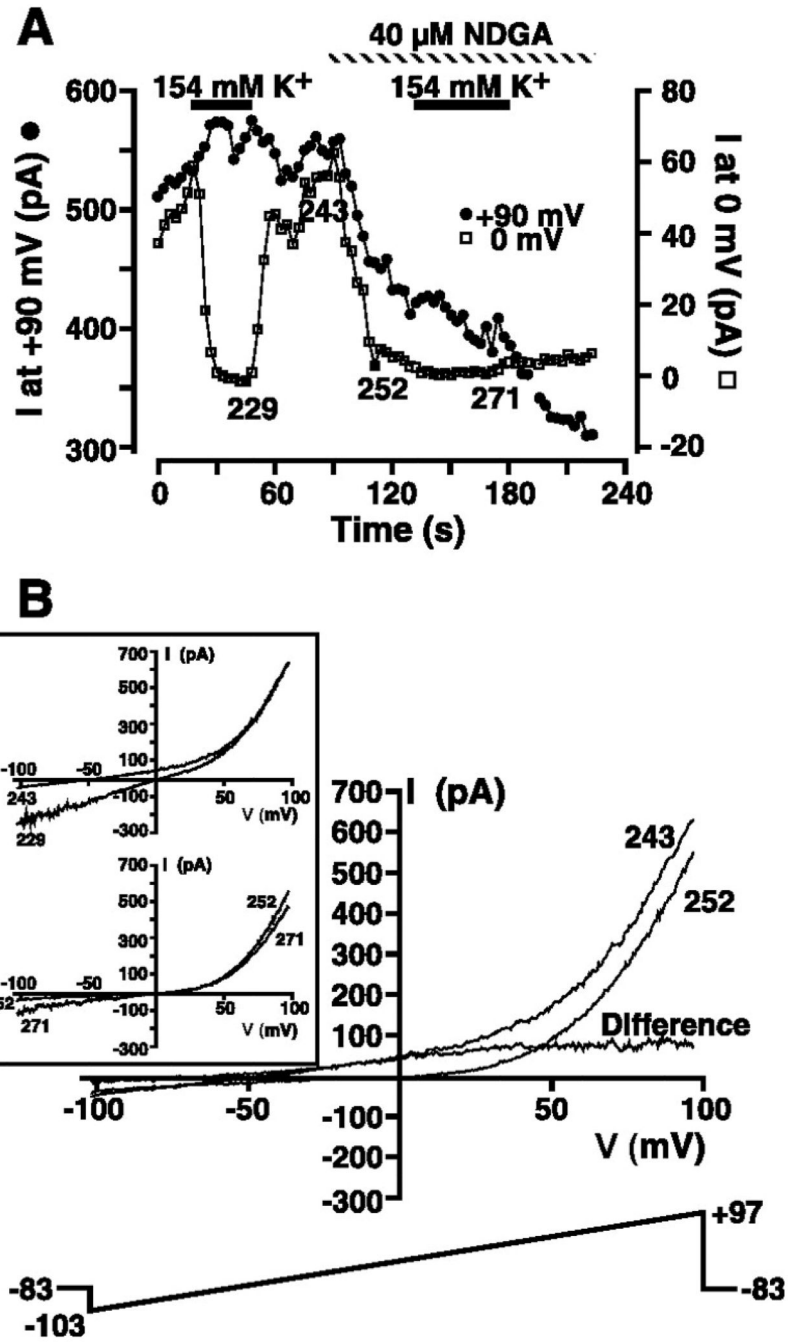

Fig. 9.

Isolation of the MIP current in low extracellular K^+ solution by NDGA inhibition. *A*: cell suspended in 149 Na^+/5 mM K^+ solution (*solution 9*) was whole cell patch-clamped with a Mg^{2+}-free KCl-based internal solution (*solution 3*). The 200-ms voltage-ramp protocol administered every 3 s is shown in *B*. Magnitude of the outward current at +90 and 0 mV was extracted from ramp data and plotted as a function of time. Where indicated, extracellular solution was changed to 154 mM K^+ (*solution 10*), and 40 μM NDGA was applied. *B*: *I-V* relationships in 149 Na^+/5 mM K^+ solution (*solution 9*) before (*episode 243*)

and shortly after (*episode 252*) application of 40 μM NDGA. *I-V* relationship labeled "Difference" was obtained by subtraction of the *I-V* relationship after NDGA addition (*episode 252*) from that before NDGA addition (*episode 243*) and is the *I-V* relationship for the MIP conductance in the absence of TRPM7 contamination. *Inset*: *I-V* relationships obtained in the presence (*episodes 229* and *271*) and absence (*episodes 243* and *252*) of high extracellular K^+ solution before and during NDGA application as denoted in *A*. Voltage-ramp protocol is shown in main panel.

Europe PMC Funders Author Manuscripts

Europe PMC Funders Author Manuscripts

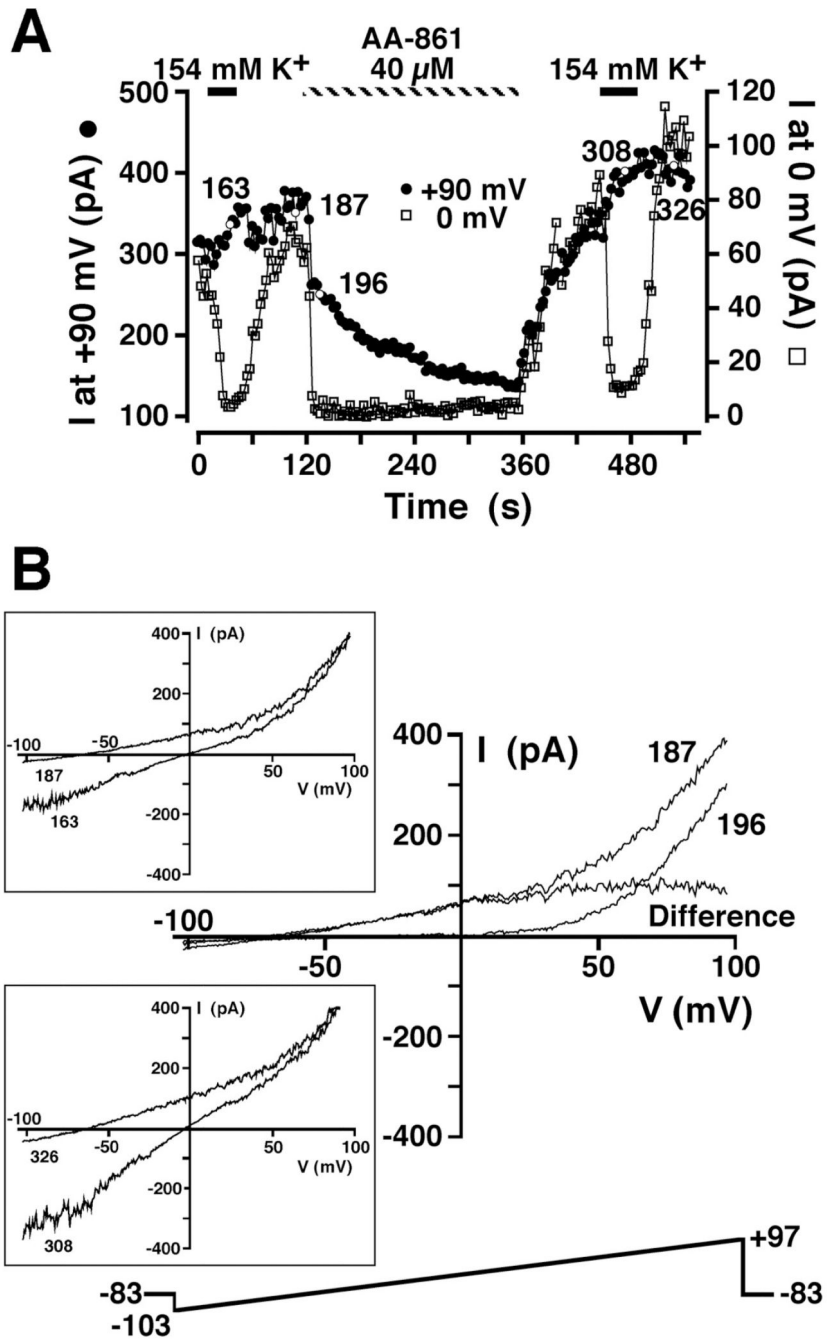

Fig. 10.

Isolation of MIP current in low extracellular K^+ solution by AA-861 inhibition. *A*: cell suspended in 149 Na^+/5 mM K^+ solution (*solution 9*) was whole cell patch-clamped with a Mg^{2+}-free KCl-based internal solution (*solution 3*). The 200-ms voltage-ramp protocol administered every 3 s is shown in *B*. Magnitude of the outward current at +90 and 0 mV was extracted from ramp data and plotted as a function of time. Where indicated, extracellular solution was changed to 154 mM K^+ (*solution 10*) and 40 μM AA-861 was applied. *B*: *I-V* relationships in 149 Na^+/5 mM K^+ solution (*solution 9*) before (*episode 187*)

and shortly after (*episode 196*) application of 40 μM AA-861. *I-V* relationship labeled "Difference" is the difference between *episodes 187* and *196* and is the *I-V* relationship for the MIP conductance in the absence of TRPM7 contamination. *Inset*: *I-V* relationships obtained in the presence (*episodes 163* and *308*) and absence (*episodes 187* and *326*) of high extracellular K^+ solution before and after AA-861 application as denoted in *A*. Voltage-ramp protocol is shown in main panel.

Europe PMC Funders Author Manuscripts

Europe PMC Funders Author Manuscripts

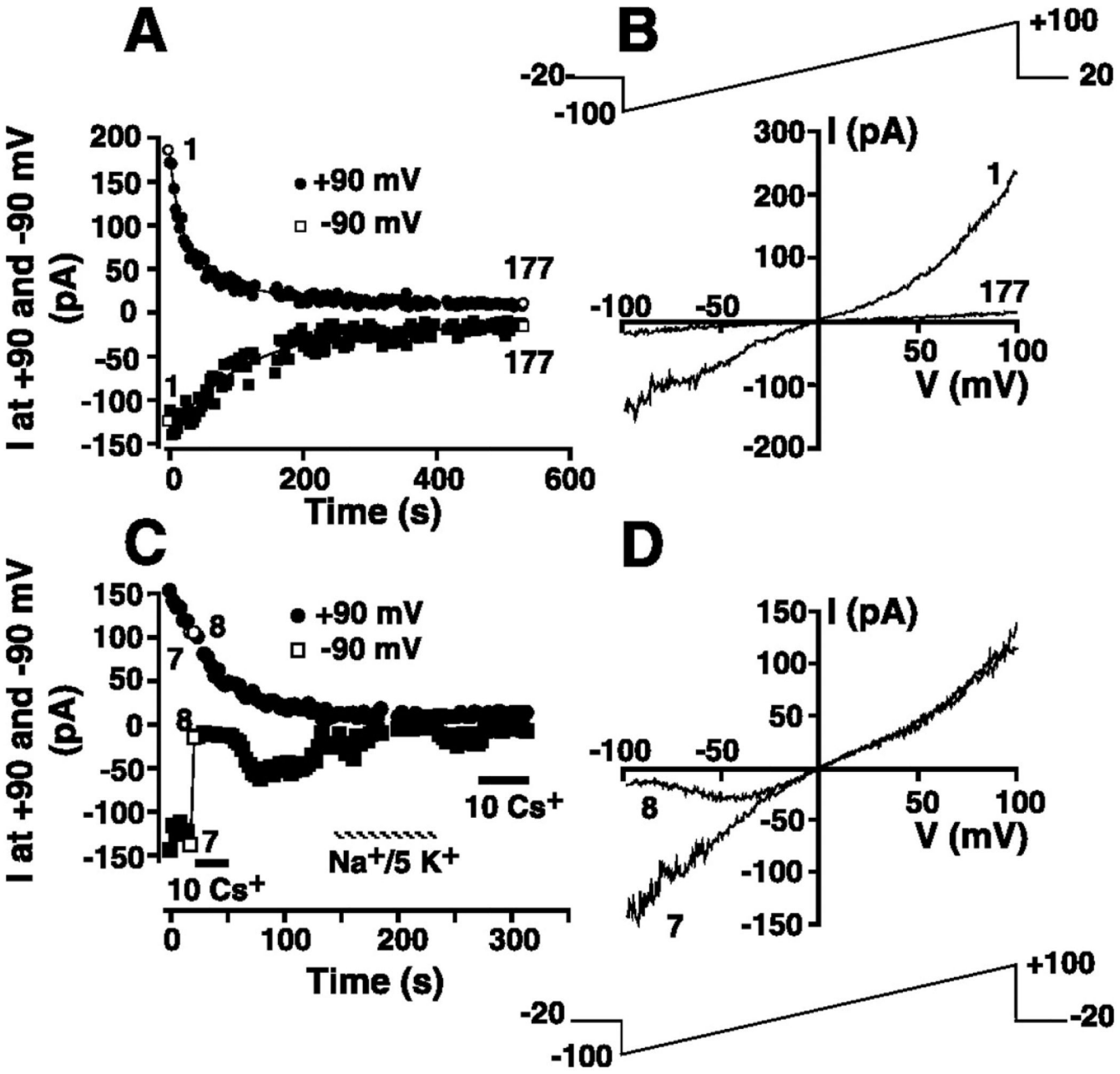

Fig. 11.

Constitutive expression of MIP and TRPM7 currents in HEL cells. *A*: cell was whole cell patch-clamped with KCl-based internal solution (*solution 1*) supplemented with 5 mM Mg^{2+} and superfused with 154 mM K^+ solution (*solution 10*). The 200-ms voltage-ramp protocol administered every 3 s is shown in *B*. Magnitude of the current at −90 and +90 mV was extracted from each ramp and plotted as a function of time. Curves are best fits of double exponentials to data. *B*: *I-V* relationships immediately after whole cell configuration was attained (*episode 1*) and 531 s later (*episode 177*). *C*: cell superfused with 154 mM K^+ solution (*solution 19*) was whole cell patch-clamped with a KCl-based internal solution (*solution 1*) supplemented with 5 mM Mg^{2+}. The 200-ms voltage-ramp protocol

administered every 3 s is shown in *D*. Magnitude of the currents at −90 and +90 mV is plotted as a function of time. Where indicated, extracellular solution was changed to 154 mM KCl (*solution 10*) supplemented with 10 mM Cs^+ or replaced with 149 Na^+/5 K^+ solution (*solution 9*). *D*: whole cell *I-V* relationships in the absence (*episode 7*) and presence (*episode 8*) of 10 mM Cs^+.

Europe PMC Funders Author Manuscripts

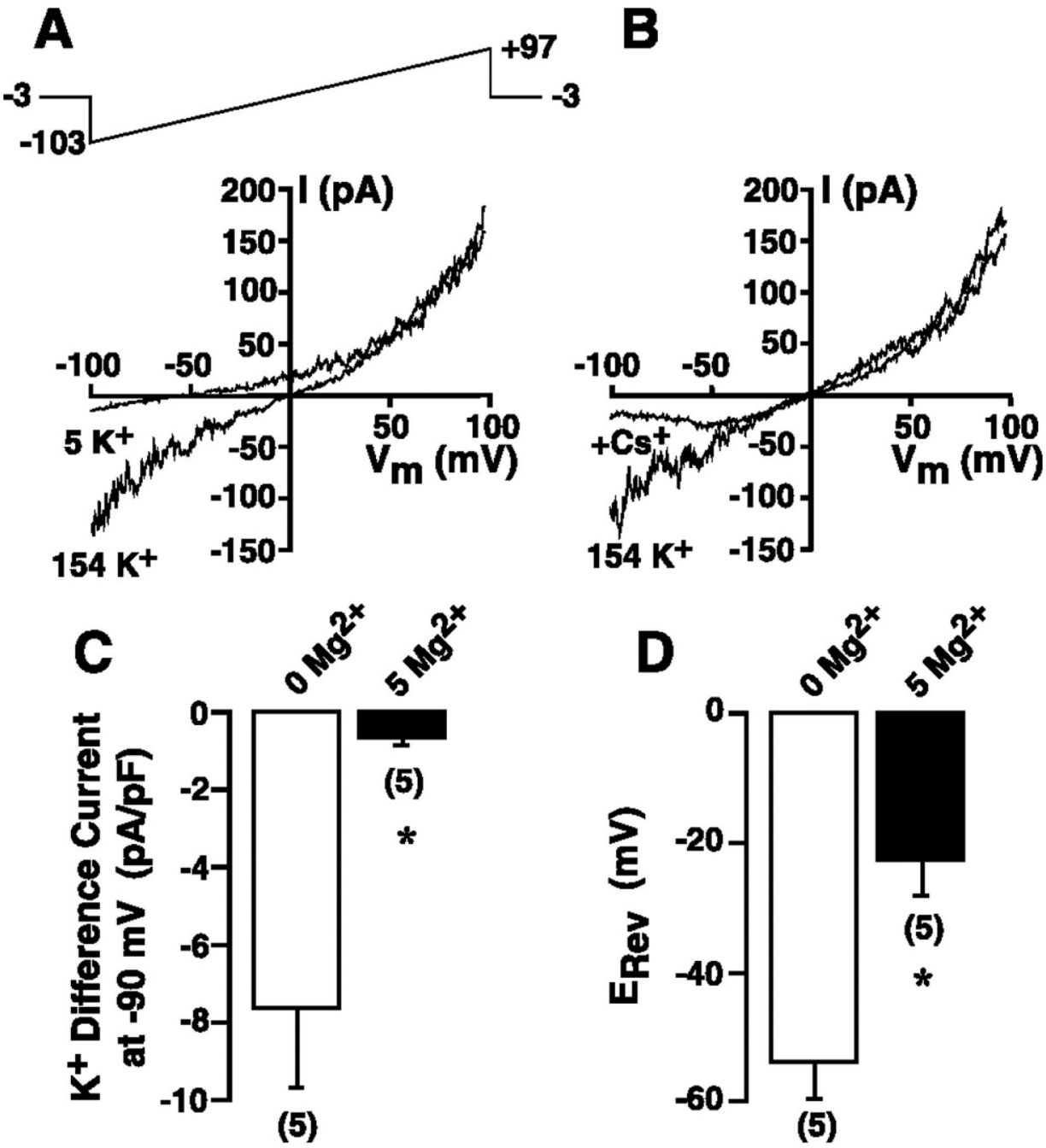

Fig. 12.

Detection of a MIP-like current in CHRF-288-11 cells. *A*: whole cell *I-V* relationship derived from voltage ramps in the presence of 149 Na^+/5 mM K^+ solution (*solution 9*) or 154 mM K^+ extracellular solution (*solution 10*). Cell was whole cell patch-clamped using a 154 mM KCl-based nominally Mg^{2+}-free pipette solution (*solution 1*), and the 200-ms voltage ramp (*top*) was administered every 3 s. *B*: cell was superfused with 154 mM K^+ solution (*solution 10*) during whole cell patch clamp using a nominally Mg^{2+}-free KCl-based internal solution (*solution 1*). Voltage-ramp protocol in *A* was carried out in the

presence and absence of 10 mM Cs^+. *C*: cells were whole cell patch-clamped with a nominally Mg^{2+}-free KCl-based internal solution (*solution 1*) or a KCl-based internal solution (*solution 1*) supplemented with 5 mM Mg^{2+}, and 200-ms voltage ramps from −103 to +97 mV were administered every 3 s from a holding potential of −3 mV. K^+ difference current was calculated as the magnitude of the current at −90 mV in 154 mM K^+ solution (*solution 10*) minus the magnitude of the current at the same potential in 149 Na^+/5 mM K^+ solution (*solution 9*) and normalized for cell capacitance. *D*: reversal potential in 149 Na^+/5 mM K^+ solution (*solution 9*) in cells dialyzed with nominally Mg^{2+}-free KCl-based internal solution (*solution 1*) or KCl-based internal solution (*solution 1*) supplemented with 5 mM free Mg^{2+}. Numbers in parentheses denote sample size. **P* ≤ 0.05 vs. 0 Mg^{2+}.

Europe PMC Funders Author Manuscripts